J. Math. Biol. (2004)
Digital Object Identifier (DOI):
10.1007/s00285-004-0295-1

Mathematical Biology

M. Scholz · C. Engel · M. Loeffler

Modelling Human Granulopoiesis under Polychemotherapy with G-CSF Support

Received: 29 January 2004 / Revised version: 19 August 2004 /
Published online: 20 December 2004 – © Springer-Verlag 2004

Abstract. Cytotoxic drugs administered in polychemotherapy cause a characteristic neutropenic period depending on the schedule of the drugs, which can partly be prevented by G-CSF growth factor support. To quantify these effects and to gain a deeper insight into the dynamics of bone marrow recovery after such suppressing and stimulating disturbances, we construct a biomathematical compartment model of human granulopoiesis under polychemotherapy with G-CSF support. The underlying assumptions and mathematical techniques used to obtain the model are explained in detail. A large variety of biological and clinical data as well as knowledge from a model of murine haematopoiesis are evaluated to construct a physiological model for humans.

Particular emphasis is placed on estimating the influence of chemotherapeutic drugs on the granulopoietic system. As a result, we present an innovative method to estimate the bone marrow damage caused by cytotoxic drugs with respect to single identifiable cell stages only on the basis of measured peripheral blood leukocyte dynamics. Conversely, our model can be used in a planning phase of a clinical trial to estimate the haematotoxicity of regimens based on new combinations of drugs already considered and with or without growth factor support.

1. Introduction, Basics of the Model and Methods

1.1. Background and Motivation

It has been shown recently ([PTK1 et al.], [PTK2 et al.], [BLG et al.]), that dose- and time-intensification of multicyclic polychemotherapy improves the therapeutic outcome for lymphomas. For a better treatment effect, the application of chemotherapeutic drugs is repeated several times in fixed time distances. On the other hand, leukopenia induced by the side effects of general cytotoxicity of drugs administered in polychemotherapy is a major limiting factor for such intensified regimen. Therefore, the granulopoietic growth factor G-CSF (granulocyte colony-stimulating factor) is often used to reduce the neutropenic period.

In order to design a chemotherapy regimen using new drugs or different drug combinations, it is necessary to estimate the myelotoxic potential. One must predict, for example, if the dosage and time schedule of the regimen results in tolerable

M. Scholz, C. Engel, M. Loeffler: University of Leipzig, Institute for Medical Informatics, Statistics and Epidemiology, Liebigstraße 27, 04103 Leipzig, Germany. e-mail: markus.scholz@imise.uni-leipzig.de

Key words or phrases: Chemotherapeutic drugs – Compartment model – Granulocyte-colony stimulating factor (G-CSF) – Haematotoxicity – Human granulopoiesis

toxicity. One may also wish to determine conditions under which optimal G-CSF application is obtained. To provide a quantitative basis for these objectives we construct a mathematical model which simulates human granulopoiesis under chemotherapy with G-CSF support and may be used to obtain such predictions.

To better understand granulopoiesis under chemotherapy, we attempt to isolate and quantify the rates of damage due to different cytotoxic drugs as a function of the administered dose. The rates we obtained are derived by fitting the predictions of our model to clinical data which record the time course of leukocytes under several established chemotherapy regimens used in various multicenter trials of the German lymphoma trial groups, in which a member of our group (M. Loeffler) is involved.

Using these rates, one should obtain reliable predictions concerning the myelotoxicity of any given chemotherapy regimen based on the cytotoxic drugs considered.

In this paper particular emphasis is placed on the underlying mathematical techniques of our modelling. Detailed clinical aspects are treated elsewhere [ESL].

1.2. Basic Model Structure

It is our major intention to construct a physiological model which can at least potentially be compared with still missing bone marrow data of humans under therapy. Furthermore, parameters of the model should have a measurable biological equivalent as far as possible. Finally, the model should map major identified regulatory mechanisms of granulopoiesis to provide a deeper insight into this complex biological process. To address these objectives, an ordinary differential equation model seemed to us appropriate.

We build a physiological compartment model including the following cell stages and cytokines which are involved in granulopoiesis.

Compartment	Meaning	Biological equivalent
S	stem cells	
CG	granulopoietic progenitor cells	CFU-GM (colony forming units of granulocytes and macrophages)
PGB	proliferating granulopoietic precursor cells	myeloblasts ($G1$), promyelocytes ($G2$), myelocytes ($G3$)
MGB	maturing granulopoietic precursor cells	metamyelocytes ($G4$), banded ($G5$) and segmented ($G6$) granulocytes
GRA	granulocytes	peripheral blood granulocytes
G	$CG \cup PGB \cup MGB$	total granulopoetic cells in bone marrow
E		total erythropoietic cells in bone marrow
$G-CSF$	G-CSF (granulocyte colony-stimulating factor)	cytokine of granulopoiesis
$GM-CSF$	GM-CSF (granulocyte, macrophage colony-stimulating factor)	”
CX	cytotoxic drugs	damage due to chemotherapy

We are interested in the time dependent behaviour of cell numbers in single compartments under the influence of chemotherapy and G-CSF administration. Therefore, we model the fluxes between cell compartments, the amplification of cell numbers within single compartments, the strength of regulatory influences of cytokines and the damaging behaviour of chemotherapeutic drugs as well (see figure 1). This leads to a system of coupled ordinary differential equations.

Based on a differential equation model of murine haematopoiesis which has already been established by us with striking success in explaining various non-pathological and pathological phenomenon in murine haematopoiesis ([WL]), we provide a similar model structure with a similar regulatory mechanism.

For the unperturbed situation of granulopoiesis we assume a steady state situation representing the fixed point of the differential equation system which is autonomous in this case.

In general, our problem is an initial value problem, where the initial values are so called normal values representing the steady state situation. Hence, these values were calculated by the condition that cell numbers do not change in each cell stage (see chapter 3). In the clinical sense this is equivalent to an unperturbed granulopoiesis in the patients at the beginning of therapy. Exceptions from this assumption are discussed in section 4.3.2.

1.3. Basic Model Assumptions

We describe the most important assumptions and simplifications, leading to the model equations:

1. Proliferation and maturation of granulopoietic cell stages are regulated by growth factor mediated feedback loops (e.g. G-CSF, GM-CSF, compare [SFL et al.]).

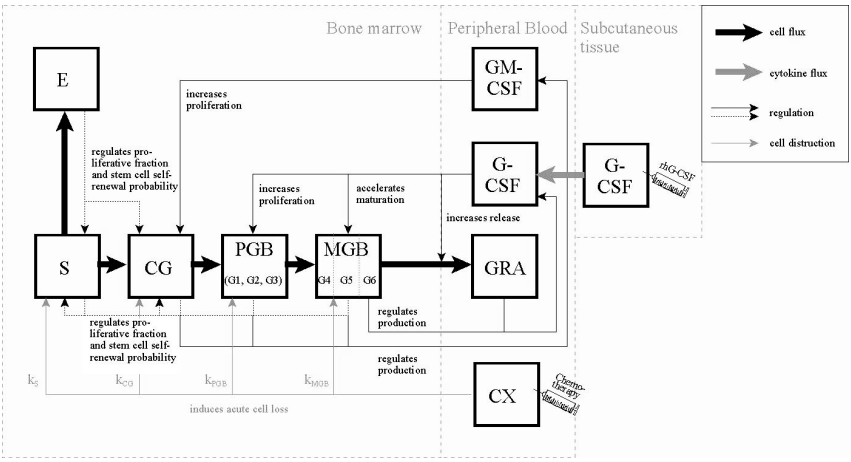

Fig. 1. Basic Model Structure.

2. G-CSF increases proliferation, shortens maturation times and increases the release of white blood cells from bone marrow to blood (e.g. [SFBW], [LBO et al.]).
3. Proliferating precursor cells are summarized in one compartment ($PGB = G1 \cup G2 \cup G3$).
4. Even though, erythropoiesis is not explicitly modeled, the indirect regulatoring influence of erythropoiesis to granulopoiesis is considered via the assumption of equal damaging and recovering behaviour of both cell lineages (see sections 2.2, 2.3).
5. Single applications of cytotoxic drugs induce an instantaneous depletion in each cell stage of bone marrow, lasting one day, according to the fast metabolism of these substances ([BBB et al.], [BCMO], [Sin]). On the other hand, toxic metabolites which could remain for a longer time, are neglected.
6. The bone marrow damage caused by chemotherapy is assumed to be reversible (compare [LS]). As a consequence, parameter settings keep unchanged after chemotherapy.
7. The damaging behaviour is assumed to follow a first order depletion of cells according to mouse data in [LS]. We define the ratio of cell loss rate to compartment size as corresponding (constant) specific toxicity parameter k (unit h^{-1}).
8. Different cytotoxic drugs damage independently from each other.

Minor assumptions especially in the context of modelling certain chemotherapy regimens are explained in the text.

1.4. Determination of Parameters

From the ethical point of view it is not possible to collect detailed bone marrow data of human granulopoiesis. Due to these missing data, the determination of parameters in the human model is more difficult than for the mouse model. Values for proliferation rates and transit times of different bone marrow cell stages are taken from the literature, but some of them are only known up to a certain range. Furthermore, model parameters regarding sensitivity of certain regulatory mechanisms (sensitivity parameters) of cytokines have no direct biological measurable equivalent. Finally, we want to apply the model to estimate single effects of cytotoxic drugs administered in chemotherapy, hence, we need to quantify corresponding parameters. A stepwise fitting procedure will be established to determine such unknown model parameters. Consequently, the model curve of peripheral blood granulocytes GRA, which is assumed to be proportional to the number of leukocytes (see [ESL]), is compared with clinical data of the time course of leukocytes of patients treated with or without G-CSF or cytotoxic drugs. We start with data obtained from a repeated administration of G-CSF to healthy volunteers. We continue with the data of different chemotherapy regimens from low to high number of administered drugs or drug combinations with or without G-CSF support, keeping already identified parameters constant in the following fitting processes.

The leukocyte data under chemotherapy were obtained from multicenter trials of the *German High Grade Non-Hodgkin's-Lymphoma Study Group* and the *German Hodgkin's Lymphoma Study Group* enclosing 2977 patients with 18565 evaluated cycles and 75598 single measurements. We consider 10 different chemotherapy protocols with up to 5 cytotoxic drugs in different application schedules (see section 4.3.1).

The fitting procedure for the chemotherapy data is based on an optimization function which represents the squared difference between the logarithms of the normalized model curve (normal value is 7000 leukocytes per μl blood) and the median of normalized clinical data to certain time points, weighted by the standard error of median of the clinical data. In order to provide an optimal fit of the nadir phase of leukocytes, we used logarithms of data instead of the original data. The standard error at a single time point represents the certainty of the corresponding data, therefore, our optimization function guarantees a better fit to data points with higher certainty. From the mathematical point of view, one obtains the following optimization problem. Let $\{t_i\}$ $(i = 1, \ldots, N)$ be the time points (here days) on which leukocyte counts were collected. Let $\tilde{x}_i$ be the median of the available normalized measurements at the time t_i, let σ_i be the standard error of the median $\tilde{x}_i$ and $f(t; \mathbf{k})$ be the solution of the model equation system for the granulocyte compartment based on the parameter set $\mathbf{k}$ then the extremal value problem

$$\sum_{i=1}^{N} \frac{1}{\sigma_i} \ln^2 \left(\frac{\tilde{x}_i}{f(t_i; \mathbf{k})} \right) \qquad \rightarrow \qquad \text{minimize with respect to } \mathbf{k}!$$

has to be solved. In the following, the left hand side is referred to as the fitness function.

Since there are only a few data points for the repeated administration of G-CSF to healthy volunteers, we used another optimization function for the fitting of such data (see section 4.1, 4.2). Here, the corresponding leukocyte and G-CSF serum level data were fitted pointwise. Let (t_i, x_i) $(i = 1, \ldots, N)$ be the time points t_i with the corresponding normalized measurements x_i (either leukocyte counts or G-CSF serum concentrations) and let $f(t; \mathbf{k})$ be again the solution of the differential equation system for the corresponding model compartment, we have to solve the following extremal value problem

$$\sum_{i=1}^{N} \ln^2 \left(\frac{x_i}{f(t_i; \mathbf{k})} \right) \qquad \rightarrow \qquad \text{minimize with respect to } \mathbf{k}!$$

To solve the problems, evolutionary strategies appeared to be the best method to obtain a global optimum as good as possible. This non-deterministic optimization method is based on the principles of evolution which are mutation by chance, reproduction, realization of phenotypes and survival of the fittest. For mathematical application, parameter settings were taken instead of livings, that is parental parameter settings are changed by chance (mutation), combined to form new settings (reproduction) and used to solve the model equation system (realization). The

parameter settings for which one obtains a good agreement between the model prediction and the data were taken to create the next generation of parameter settings (survival of the fittest). The fitness function is a measure for this agreement. See also [R], [Sch] for further details of evolutionary strategies.

Experimentally, we identified (1+5) and (1,5) evolutionary strategies with self-adapting mutation step size as best algorithms for our problem. Consequently, one of these strategies had been used in most of our fitting procedures. According to [R], (1+5) is an evolution with one possibly immortal parent having five children and (1,5) means that the parent dies after reproduction and cannot produce any further generation. Depending on the number of parameters which are fitted, we needed between approximately 100 generations for 2 parameter fittings to a few thousand generations for a maximum of a 22 parameter fitting to stabilize the evolution algorithm.

Summarizing the above discussion, the following procedure for the determination of model parameters is used.

1. Most of the parameters were obtained from the literature, partly adopted from an earlier model of human granulopoiesis (see [SFBW]) based on a collection of measured granulopoietic quantities.
2. Some parameters, especially weighting factors and parameters related to stem cell regulation, were adopted from the corresponding mouse model [WL].
3. In the case of available but uncertain values, the parameters were fitted within the predicted range.
4. Parameters with no available data or without a direct biological meaning were denoted "speculative". These parameters were fitted or set in dependence on the model sensitivity with respect to changes of this quantity. The number of these parameters has been kept as small as possible, either by making simple assumptions or by keeping corresponding regulatory mechanisms constant or by equating related parameters (e.g. sensitivity parameters for transit time in subcompartments of MGB, see appendix) to prevent over-fitting of data.

We provide a complete parameter list for our model in the appendix of this paper.

1.5. Simulation and Numerical Methods

Our model has been programmed with MATLAB 5.2.0.3084 and SIMULINK toolbox (The MathWorks Inc., Natick, MA, USA). Simulations of the model were performed by numerical integration of the equation system using the variable step solver from Adams and Bashford implemented in the SIMULINK toolbox.

2. Regulatory Mechanisms of the Model

2.1. Overview over the most important state variables

The following table provides a list of the model state variables for a better understanding of the model equations.

quantity	meaning	type/calculation
C_X	(normalized) content of compartment X	function of time t
C_X^{nor}	content of compartment X in steady state (normal value)	parameter, in general we set $C_X(0) = C_X^{nor}$ [1]
C_X^{rel}	content of compartments X relative to normal value	$C_X^{rel}(t) = \frac{C_X(t)}{C_X^{nor}}$
C_X^{in}	influx in compartment X	function of time
$C_X^{in\_nor}$	normal influx	parameter, see above
C_X^{out}	efflux from compartment X	function of time
$C_X^{out\_nor}$	normal efflux	parameter, see above
a_X	proliferative fraction in cell compartment X	function of state, sometimes constant
A_X	amplification in cell compartment X	”
A_X^{in}	amplification of influx (see section 2.5.)	”
A_X^{out}	amplification of efflux (see section 2.5.)	”
n_X	average number of mitoses in cell compartment X	$n_X = \mathrm{ld}\, A_X$
p	self-renewal probability of stem cells	function of state
P_X^{endo}	endogenous production of cytokin X	”
P_X^{exo}	exogenous donation of cytokin X	given function of time
τ_X	average duration of cell cycle in compartment X	function of time, sometimes constant (not regulated)
T_X	average transit time of active cells in cell compartment X	$T_X = n_X \tau_X$
T_X^t	total transit time	$T_X^t = \frac{n_X \tau_X}{a_X}$
k	transition, degradation or toxicity coefficients	functions of time or parameter
Y^{min}	quantity Y under minimum stimulation	parameter to determine the regulatory function of Y
Y^{nor}	quantity Y in steady state	”
Y^{int}	quantity Y under intensified stimulation	”
Y^{max}	quantify Y under maximum stimulation	”
b_Y	sensitivity of Y under stimulation	”

2.2. *Self-Renewal Probability p*

According to the stem cell model of [WL] this stem cell quantity is regulated by the demand of the total haematopoietic bone marrow system.

$$p = F\left(C_S^{rel}(t),\ C_E^{rel}(t),\ C_G^{rel}(t);\ p_\delta,\ \vartheta_E,\ \vartheta_G\right)$$

The parameters ϑ_E, ϑ_G and the later described quantity ϑ_S are hypothetical weighting factors representing the influence of the corresponding compartment ([WL],

[1] As already mentioned, we assume that at $t = 0$ we have normal system values which are considered to be constant (steady state). Later, this provides formulas for the initial values. If one wants to start from a perturbed system, these formulas and initial values have to be modified.

p. 62). Further, it is assumed that $p_\delta = p^{nor} - p^{min} = p^{max} - p^{nor}$, according to [WL].

$$\vartheta_S(t) = \begin{cases} \frac{2}{C_S^{rel}(t)^{0.6}} & \text{for } C_S^{rel} \le 1 \\ 2 & \text{for } C_S^{rel} > 1 \end{cases}$$

$$\begin{aligned} p = p_\delta \tanh\Big(& -\vartheta_S(t)\left(C_S^{rel}(t) - 1\right) \\ & -\vartheta_E\left(C_E^{rel}(t) - 1\right) - \vartheta_G\left(C_G^{rel}(t) - 1\right)\Big) + 0.5 \end{aligned} \tag{1}$$

Thereby, the last equation describes a regulatory function, regulating the quantity p monotonically between p^{min} and p^{max}.

According to our simplification 4 (see section 1.3), we do not calculate the function $C_E^{rel}(t)$ explicitly to avoid the inclusion of a human erythropoiesis model with further speculative parameteres. We set $C_E^{rel}(t) = C_G^{rel}(t)$ which recognizes the changing influence of erythropoiesis to granulopoiesis due to chemotherapeutic bone marrow damage of erythropoietic cell stages. Hence, the last equation can be simplified:

$$p = p_\delta \tanh\left(-\vartheta_S(t)\left(C_S^{rel}(t) - 1\right) - (\vartheta_E + \vartheta_G)\left(C_G^{rel}(t) - 1\right)\right) + 0.5 \tag{2}$$

2.3. Proliferative Fraction a_X

This quantity occuring in different proliferative compartments is regulated by the complete haematopoietic system as well. It can be interpreted biologically as the fraction of cells of the corresponding stage which are currently in cell cycle.

$$a_X = F\left(C_S^{rel}(t),\, C_E^{rel}(t),\, C_G^{rel}(t);\, a_X^{min},\, a_X^{nor},\, a_X^{int},\, a_X^{max},\, \omega_S,\, \omega_E,\, \omega_G\right)$$

The parameters ω are weighting factors analogous to 2.2.

$$\begin{aligned} x = {} & \omega_E \ln C_E^{rel}(t) + \omega_G \ln C_G^{rel}(t) \\ & + \omega_s \cdot \begin{cases} \ln C_S^{rel}(t) & \text{for } C_S^{rel} \le 1 \\ C_S^{rel}(t) - 1 & \text{for } C_S^{rel} > 1 \end{cases} \end{aligned} \tag{3}$$

$$\begin{aligned} y = {} & -\frac{1}{2\ln 2}\left(\ln\left(\frac{a_X^{int} - a_X^{max}}{a_X^{min} - a_X^{int}}\right) - \ln\left(\frac{a_X^{nor} - a_X^{max}}{a_X^{min} - a_X^{nor}}\right)\right) x \\ & + \frac{1}{2}\ln\left(\frac{a_X^{nor} - a_X^{max}}{a_X^{min} - a_X^{nor}}\right) \end{aligned} \tag{4}$$

$$a_X = \begin{cases} \frac{a_X^{max} e^{-y} + a_X^{min} e^{y}}{e^{-y} + e^{y}} & \text{for } a_X^{min} < a_X^{nor} < a_X^{int} < a_X^{max} \\ a_X^{nor} & \text{for } a_X^{min} = a_X^{nor} = a_X^{int} = a_X^{max} \end{cases}. \tag{5}$$

This regulation has also been taken from [WL], p. 65. It is a monotone function with range domain between a_X^{min} and a_X^{max}. Hereby, low cell numbers in compartments cause a higher demand of proliferating cells and therefore an increase of a_X.

Thereby, the value of y defines the actual point on the regulatory curve. The variable x represents some kind of weighted logarithmic relative system size. In this context, the proliferative fraction a^{int} corresponds to $x = -\ln 2$ and a^{nor} corresponds to $x = 0$.

2.4. Z-Function

The Z-function is an additional regulatory function which monotonically regulates a quantity (here amplification or transit time) between the maximum and the minimum stimulation respectively, depending on the concentration of corresponding growth factors C_X (X = G-CSF or X = GM-CSF).

Another application of this function appears in the model of endogenous cytokine production (see section 3.6, 3.7) which is a function of certain cell demands.

$$Y = Z_Y\left(C_X^{rel}(t);\ Y^{min},\ Y^{nor},\ Y^{max},\ b_Y\right) \tag{6}$$

$$Z_Y\left(C_X^{rel}\right) = \begin{cases} Y^{max} - \left(Y^{max} - Y^{min}\right) e^{-\ln\left(\frac{Y^{max}-Y^{min}}{Y^{max}-Y^{nor}}\right)\left(C_X^{rel}\right)^{b_Y}} \\ \qquad\qquad \text{for } Y^{min} < Y^{nor} < Y^{max} \text{ or } Y^{min} > Y^{nor} > Y^{max} \\ Y^{nor} \quad \text{for } Y^{min} = Y^{nor} = Y^{max} \end{cases}. \tag{7}$$

2.5. Amplification Splitting

The (average) amplification rate of a cell can be interpreted as the ratio of cell efflux and cell influx in steady state caused by cell divisions taking place in the corresponding compartment. But in general while staying in one compartment, this rate can change. Since the amplification is distributed over the age levels in the compartment, a multiplication of one age group with the full new amplification rate would lead to an unrealistic, immediate change of compartment size and/or efflux size. To avoid such an effect, we use a so called amplification splitting. Therefore, influx and efflux of cells at one compartment will be amplified in a certain ratio, so that the product is the actual over-all amplification ($A_X^{in}(t) \cdot A_X^{out}(t) = A_X(t)$). The ratio of A_X^{in} and A_X^{out} will be determined by the condition, that the size of the compartment shall be constant ($\dot{C}_X = 0$) in steady state, and, that under constant amplification, the size of cell generation with age in $((k-1)\,\tau_X, k\tau_X]$ with $k \in \mathbb{N}^+$, $k \leq n_X$ is equal to the theoretical size of cell generation obtained from a cell cycle time τ_X without any variance (step function).

The major effect of amplification splitting is a delayed reaction of the system (efflux and compartment size) to changes in amplification rates, in better accordance to the observed behaviour.

Derivation of Splitting Formula: We assume that the amplification of incoming cell generations after the time t is a function of the form $f_X(t) = ae^{bt}$. In steady

state it holds, that the integral of amplified influxes over the transit time is equal to the compartment size:

$$C_X^{in} \int_0^{n_X \tau_X} f_X(t)\, dt = C_X.$$

If the cell cycle time is without any variance, we would have the theoretical amplification function:

$$f_X^{theo}(t) = \begin{cases} 1 & \text{for } t \in (0, \tau_X) \\ 2 & \text{for } t \in (\tau_X, 2\tau_X) \\ \vdots & \vdots \\ 2^{n_X - 1} & \text{for } t \in ((n_X - 1)\,\tau_X, n_X \tau_X) \end{cases}$$

and from the geometrical series we get the relation

$$\left(2^{n_X} - 1\right) \tau_X C_X^{in} = C_X$$

which is equivalent to equation (11a) in [WL], p. 59. Hence, it follows for our amplification function f that:

$$\begin{aligned} \int_0^{n_X \tau_X} f_X(t)\, dt &= \left(2^{n_X} - 1\right) \tau_X \\ \frac{a}{b} \left(e^{b n_X \tau_X} - 1\right) &= \left(2^{n_X} - 1\right) \tau_X. \end{aligned}$$

Since this equation should hold for arbitrary cell cycle times it can be concluded that $a = \ln 2$, $b = \frac{\ln 2}{\tau_X}$, consequently,

$$f_X(t) = \ln 2 \cdot 2^{\frac{t}{\tau_X}}.$$

For $t = \alpha \tau_X$ we determine α so that the theoretical amplification curve is equal to f_X ($0 < m \leq n_X, m \in \mathbb{N}^+$):

$$\begin{aligned} \ln 2 \cdot 2^{\alpha} &= 2^{m-1} \\ \Rightarrow \qquad \alpha &= m - 1 - \frac{\ln \ln 2}{\ln 2}, \end{aligned}$$

that is, at time intervals $\left((m-1)\,\tau_X\,,\ \left(m - 1 - \frac{\ln \ln 2}{\ln 2}\right) \tau_X\right)$ we have an under-estimation of amplification and at time intervals $\left(\left(m - 1 - \frac{\ln \ln 2}{\ln 2}\right) \tau_X\,,\ m \tau_X\right)$ an over-estimation of amplification which balance each other on average. Now we have for the total amplification

$$\begin{aligned} 2^{\frac{T_X}{\tau_X}} &= A_X \\ \Rightarrow \quad \tau_X &= \frac{T_X}{\mathrm{ld}\, A_X}. \end{aligned}$$

In the case of constant compartment size in steady state it shall hold:

$$\begin{aligned} C &= A_X^{in} C_X^{in} T_X \quad \text{and} \\ C &= C_X^{in} \int_0^{T_X} f_X(t)\, dt \\ \Rightarrow \quad A_X^{in} T_X &= \ln 2 \int_0^{T_X} 2^{\frac{\mathrm{ld}\, A_X}{T_X} t}\, dt \\ &= \frac{T_X}{\mathrm{ld}\, A_X} (A_X - 1)\,. \end{aligned}$$

Consequently, we have for A_X^{in} and A_X^{out}:

$$A_X^{in} = \begin{cases} \frac{A_X - 1}{\mathrm{ld}\, A_X} & \text{for } A_X \neq 0, \quad A_X \neq 1 \\ \ln 2 & \text{for } A_X = 1 \\ 0 & \text{for } A_X = 0 \end{cases} \tag{8}$$

$$A_X^{out} = \begin{cases} \frac{A_X}{A_X^{in}} & \text{for } A_X \neq 0 \\ 0 & \text{for } A_X = 0 \end{cases}. \tag{9}$$

The initial and normal values were calculated analogously to equations (8) and (9) ($A_X^{in}(0) = A_X^{in\_nor}$ and $A_X^{out}(0) = A_X^{in\_nor}$).

2.6. Division into Subcompartments

The maturation of cells and the transition between maturing compartments is neither a random transition without dependence of cell age like obeying an exponential distribution nor a strict transition with fixed time delay. More plausible is a unimodal distribution of the transit time like a Gamma-distribution. On the other hand, the problem of missing data on the variance arises.

In our model we assume in the compartment MGB a Gamma-distribution of transit time. Therefore, we divide the compartment into N cascaded subcompartments with an exponentially distributed transit time with expectation $\frac{T}{N}$. As a concequence, the transit time of the MGB compartment is Gamma-distributed with expectation T and variance $\frac{T^2}{N}$.

Proof. More generally, we prove that a cascadation of N exponentially distributed subcompartments with expectation $\frac{1}{\lambda}$ yields a Gamma-distributation with expectation $\frac{N}{\lambda}$ and variance $\frac{N}{\lambda^2}$.

The probability densities in the N subcompartments are:

$$\begin{aligned} w_1(t_1) &= \lambda e^{-\lambda t_1} \\ &\vdots \\ w_N(t_N) &= \lambda e^{-\lambda t_N}. \end{aligned}$$

We determine the probability density $w\left(t_g\right)$ for the over-all compartment, that is, with transit time $t_1 + \ldots + t_N = t_g$. Therefore, we integrate over the number of

distribution possibilities of the transit time in single compartments, so that the total transit time t_g results. Since the transit times are stochastically independent, single densities can be multiplied.

$$\begin{aligned} w\left(t_g\right) &= \int_0^{t_g} \int_0^{t_g - t_1} \cdots \int_0^{t_g - \sum_{i=1}^{N-2} t_i} \lambda e^{-\lambda t_1} \lambda e^{-\lambda t_2} \cdot \ldots \cdot \lambda e^{-\lambda t_{N-1}} \\ &\quad \cdot \lambda e^{-\lambda\left(t_g - \sum_{i=1}^{N-1} t_i\right)} dt_{N-1} \cdots dt_1 \\ &= \lambda^N e^{-\lambda t_g} \alpha_{N-1}, \end{aligned}$$

where $\alpha_{N-1} = \int_0^{t_g} \int_0^{t_g - t_1} \cdots \int_0^{t_g - \sum_{i=1}^{N-2} t_i} dt_{N-1} \cdots dt_1$. It holds that $\alpha_{N-1} = \frac{1}{(N-1)!} t_g^{N-1}$ which can be proven by induction. Obviously, the formula holds for $N = 2$. From the validity for $N - 2$ we conclude the validity for $N - 1$:

$$\alpha_{N-1} = \int_0^{t_g} \int_0^{t_g - t_1} \cdots \int_0^{t_g - \sum_{i=1}^{N-2} t_i} dt_{N-1} \cdots dt_1.$$

Substituting $\tilde{t} = t_g - t_1$, it can be derived that:

$$\alpha_{N-1} = \int_{t_g}^{0} \int_0^{\tilde{t}} \int_0^{\tilde{t} - t_2} \cdots \int_0^{\tilde{t} - \sum_{i=2}^{N-2} t_i} dt_{N-1} \cdots dt_2 d\left(t_g - \tilde{t}\right).$$

Using the proposition of the induction we get:

$$\begin{aligned} \alpha_{N-1} &= \int_0^{t_g} \frac{\tilde{t}^{N-2}}{(N-2)!} d\tilde{t} \\ &= \frac{t_g^{N-1}}{(N-1)!} \\ w\left(t\right) &= \frac{\lambda^N}{(N-1)!} t^{N-1} e^{-\lambda t} \end{aligned}$$

which is a Gamma-density.

With the special choise $\lambda = \frac{N}{T}$ we obtain a Gamma-distribution with expectation T and variance $\frac{T^2}{N}$. □

For $N = 1$ we obtain the limit case of a completely age-independent maturation process and for $N \to \infty$ a strict deterministic maturation time ("first in first out kinetic") T.

Remark. Our method estimates a variance of transit time via the parameter N. The idea of a division into subcompartments can be traced back to TAKAHASHI ([T1], [T2]).

2.7. Postmitotic Apoptosis

We assume the effect of *postmitotic depletion* in the MGB compartment, which at first has been postulated in [E], p.68, and has been measured recently in [MAD]. Since the life expectancy of granulocytes is comparatively small, a large number of cells are degraded by apoptosis while maturing. It has been shown in [CRP et al.] that G-CSF prolonges the half life of granulocytes *in vitro*. Therefore, we assume that with elevated G-CSF serum level, more granulocytes can survive the (also shortened) maturation process which provides a greater efflux of cells from bone marrow to blood. In the model this is expressed as a regulated depletion of cells in MGB depending on the G-CSF serum concentration. This process acts very short-termed and is denoted as the *release of the bone marrow reserve pool*.

Even though we fitted the postmitotic apoptosis rate in normal granulopoiesis to our data obtaining a value of 57.23% (see appendix $1 - A_{G6}^{nor}$), this quantity has been measured recently in [MAD] to be 55% which is a nearly perfect agreement with our estimate.

However, the half life of peripheral blood granulocytes *in vivo* is not prolonged by G-CSF (e.g. [SFBW], p.756), and therefore, it is unaffected by G-CSF in the model.

3. Model of Human Granulopoiesis

In this chapter, we introduce the equations which prescribe the behaviour of the single compartments. Generally, the differential equations for the compartment sizes are balance equations of the schematic form

$$\text{change of compartment size} = \text{influx} \cdot \text{amplification} - \text{efflux} - \text{cell loss}$$

In general, the initial values for this initial value problem are normal values (see chapter 1). The same is true for each other time-dependent quantity (a_X, A_X, p, T_X). Parameters are specified in the appendix, except for the toxicity parameters k_X which are specified in chapter 4.

3.1. S

$$\frac{d}{dt}C_S = (2p-1)\,C_S\frac{a_S}{\tau_S} - k_S\Psi_{CX}C_S \tag{10}$$

$$C_S^{out} = 2\,(1-p)\,C_S\frac{a_S}{\tau_S} \tag{11}$$

The function Ψ_{CX} is the characteristic chemotherapy function. Let $\{t_i\}$ $(i = 1, \ldots, M)$ be the time points of administration of cytotoxic drugs after the beginning of chemotherapy in ascending order ($t_i \in \mathbb{N}$ in days). According to section 1.3 assumption 5, the characteristic chemotherapy function is defined by

$$\Psi_{CX}(t) = \begin{cases} 1 & \text{if } \exists i \ : \ (t > t_i) \wedge (t - t_i \leq 1) \\ 0 & \text{else} \end{cases}. \tag{12}$$

Initial values: Since $p = \frac{1}{2}$ in steady state, equation 10 does not provide a normal value. We set $C_S^{nor} = 1$ which is a general normalization of cell numbers. Because of the linearity of the balance equations with respect to the compartment size and the fact that the cell number arguments of regulatory functions are also normalized, realistic cell numbers could easily be obtained by an adequat change of this quantity.

$$C_S(0) = C_S^{nor} = 1 \tag{13}$$

$$C_S^{out}(0) = C_S^{out\_nor} = 2\left(1 - p^{nor}\right) C_S^{nor} \frac{a_S^{nor}}{\tau_S} \tag{14}$$

3.2. CG

$$A_{CG} = Z_{A_{CG}}\left(C_{GM-CSF}^{rel}\right) \tag{15}$$

$$\frac{d}{dt}C_{CG} = \alpha_G C_S^{out} A_{CG}^{in} - C_{CG}\frac{a_{CG}}{T_{CG}} - k_{CG}\Psi_{CX}C_{CG} \tag{16}$$

$$C_{CG}^{out} = C_{CG} A_{CG}^{out} \frac{a_{CG}}{T_{CG}} \tag{17}$$

The quantity α_G denotes the ratio of stem cells which differentiate into the granulopoietic lineage. We assume α_G to be constant. Since we are calculating always with relative compartment sizes, this constant has no influence on the solution and can be set to one without any restriction ($\alpha_G = 1$).

Initial values:

$$C_{CG}(0) = C_{CG}^{nor} = C_S^{out\_nor} A_{CG}^{in\_nor} \frac{T_{CG}^{nor}}{a_{CG}^{nor}} \tag{18}$$

$$\begin{aligned} C_{CG}^{out\_nor} &= C_{CG}^{nor} A_{CG}^{out\_nor} \frac{a_{CG}^{nor}}{T_{CG}^{nor}} \\ &= C_S^{out\_nor} A_{CG}^{nor} \\ C_{CG}^{out}(0) &= C_{CG}^{out\_nor} = C_S^{out\_nor} A_{CG}^{nor} \end{aligned} \tag{19}$$

3.3. PGB

$$A_{PGB} = Z_{A_{PGB}}\left(C_{G-CSF}^{rel}\right) \tag{20}$$

$$\frac{d}{dt}C_{PGB} = C_{CG}^{out} A_{PGB}^{in} - C_{PGB}\frac{a_{PGB}}{T_{PGB}} - k_{PGB}\Psi_{CX}C_{PGB} \tag{21}$$

$$C_{PGB}^{out} = C_{PGB} A_{PGB}^{out} \frac{a_{PGB}}{T_{PGB}} \tag{22}$$

Initial values:

$$C_{PGB}(0) = C_{PGB}^{nor} = C_{CG}^{out\_nor} A_{PGB}^{in\_nor} \frac{T_{PGB}^{nor}}{a_{PGB}^{nor}} \tag{23}$$

$$C_{PGB}^{out}(0) = C_{PGB}^{out\_nor} = C_{CG}^{out\_nor} A_{PGB}^{nor} \tag{24}$$

3.4. MGB

As already mentioned, this compartment is divided into $G4$, $G5$ and $G6$ which again are divided into N_X subcompartments to account for the Gamma-distributed transit time delay (see section 2.6). In these subcompartments, the effect of postmitotic depletion (see section 2.7) has already been implemented and is denoted again with A for simplicity.

$$C_{MGB} = C_{G4} + C_{G5} + C_{G6} \tag{25}$$
$$C^{out}_{MGB} = C^{out}_{C6} \tag{26}$$

Initial values:

$$C_{MGB}\,(0) = C^{nor}_{MGB} = C^{nor}_{G4} + C^{nor}_{G5} + C^{nor}_{G6} \tag{27}$$
$$C^{out}_{MGB}\,(0) = C^{out\_nor}_{MGB} = C^{out\_nor}_{C6} \tag{28}$$

3.4.1. G4

$$A_{G4} = Z_{A_{G4}}\left(C^{rel}_{G-CSF}\right) \tag{29}$$
$$T_{G4} = Z_{T_{G4}}\left(C^{rel}_{G-CSF}\right) \tag{30}$$
$$C_{G4} = \sum_{i=1}^{N_{G4}} C_{G4\_i} \tag{31}$$
$$\frac{d}{dt}C_{G4\_1} = C^{out}_{PGB} - C_{G4\_1}\frac{N_{G4}}{T_{G4}} - k_{MGB}\Psi_{CX}C_{G4\_1} \tag{32}$$
$$\frac{d}{dt}C_{G4\_i} = C^{out}_{G4\_(i-1)} - C_{G4\_i}\frac{N_{G4}}{T_{G4}} - k_{MGB}\Psi_{CX}C_{G4\_i} \qquad \text{for } i = 2, \ldots, N_{G4} \tag{33}$$
$$C^{out}_{G4\_i} = A_{G4\_i}C_{G4\_i}\frac{N_{G4}}{T_{G4}} \qquad \text{for } i = 1, \ldots, N_{G4} \tag{34}$$
$$C^{out}_{G4} = C^{out}_{G4\_N_{G4}} \tag{35}$$

Remark. The total postmitotic depletion $A_{G4} \leq 1$ is equally distributed over all subcompartments in which there is postmitotic depletion, for example, if there is postmitotic depletion in all subcompartments, it holds that $A_{G4\_i} = {A_{G4}}^{1/N_{G4}}$. In our model we choose $N_{G4} = 5$, the same is true for N_{G5}, N_{G6} (see section 3.4.2., 3.4.3. and appendix).

Initial values:

$$C_{G4}(0) = C_{G4}^{nor} = \sum_{i=1}^{N_{G4}} C_{G4\_i}^{nor} \tag{36}$$

$$C_{G4\_1}(0) = C_{G4\_1}^{nor} = C_{PGB}^{out\_nor} \frac{T_{G4}^{nor}}{N_{G4}} \tag{37}$$

$$\begin{aligned} C_{G4\_i}(0) &= C_{G4\_i}^{nor} = C_{G4\_(i-1)}^{out\_nor} \frac{T_{G4}^{nor}}{N_{G4}} \\ &= C_{PGB}^{out\_nor} \frac{T_{G4}^{nor}}{N_{G4}} \prod_{j=1}^{i-1} A_{G4\_j}^{nor} \qquad \text{for } i = 2, \ldots, N_{G4} \end{aligned} \tag{38}$$

$$C_{G4\_i}^{out}(0) = C_{G4\_i}^{out\_nor} = C_{G4\_i}^{nor} A_{G4\_i}^{nor} \frac{N_{G4}}{T_{G4}^{nor}} \qquad \text{for } i = 1, \ldots, N_{G4} \tag{39}$$

$$C_{G4}^{out}(0) = C_{G4}^{out\_nor} = C_{G4\_N_{G4}}^{out\_nor} \tag{40}$$

3.4.2. G5

The corresponding formulas are identical to (29) to (40) if $G4$ is replaced by $G5$ and PGB is replaced by $G4$.

3.4.3. G6

The corresponding formulas are identical to (29) to (40) if $G4$ is replaced by $G6$ and PGB is replaced by $G5$.

3.5. GRA

$$\frac{d}{dt} C_{GRA} = C_{MGB}^{out} - C_{GRA} \frac{1}{T_{GRA}} \tag{41}$$

Here, we assume that the degradation of granulocytes is an age-independent random process. Therefore, the transit time parameter T can be understood as the expected value of the corresponding exponential distribution. The same is true for the degradation mechanisms of the cytokines (see next sections). However, in literature the concept of half life $t_{1/2}$ is more common in the context of such processes. With the relation $t_{1/2} = (\ln 2)T$ one can transform easily between these two quantities.

In some chemotherapies the steroid prednisone is administered as a supportive therapy. It is well known that prednisone prolonges the half life (and therefore also the transit time) of granulocytes (see [BAB et al.], [DFW]). We define

$$T_{GRA} = T_{GRA}^{nor} \left(1 + T_{GRA}^{Pred} \Psi_{Pred}\right), \tag{42}$$

where T_{GRA}^{Pred} represents the percentage of prolongation of the transit time and Ψ_{Pred} is the characteristic function of prednisone administration. According to [DFW],

it is analogously defined as the characteristic function of chemotherapy (equation (12)), that is, the prednisone effect stops also one day after administration in our model.

Initial value:

$$C_{GRA}(0) = C_{GRA}^{nor} = C_{MGB}^{out\_nor} T_{GRA} \tag{43}$$

3.6. GM-CSF

The regulation of endogenous production of GM-CSF and G-CSF is not very well understood [HH]. It is known to be correlated with the demand for mature granulocytes [LRO]. In our production models, we assume that production is a function of the bone marrow status of granulopoiesis which is an indirect measure of that quantity.

$$P_{GM-CSF}^{endo} = Z\left(\frac{w_{CG}C_{CG} + w_{PGB}C_{PGB} + w_{G4}C_{G4} + w_{G5}C_{G5} + w_{G6}C_{G6}}{w_{CG}C_{CG}^{nor} + w_{PGB}C_{PGB}^{nor} + w_{G4}C_{G4}^{nor} + w_{G5}C_{G5}^{nor} + w_{G6}C_{G6}^{nor}}\right) \tag{44}$$

$$\frac{d}{dt}C_{GM-CSF} = P_{GM-CSF}^{endo} - C_{GM-CSF}\frac{1}{T_{GM-CSF}} \tag{45}$$

The quantities w_X are hypothetical weighting factors (see appendix), representing the influence of each cell stage on the production of GM-CSF. There are no direct biological data available to support the specific choice of the weighting factors as well as for the weighting factors for the G-CSF production (see next section). However, these settings were appropriate in our former models of cyclic neutropenia in dogs and children ([SLJ et al.], [SFL et al.]). We kept these parameters constant to ensure consistency with these models. A sensitivity analysis also showed, that the model behaviour is not very sensitive with respect to changes of these quantities.

Initial value:

$$C_{GM-CSF}(0) = C_{GM-CSF}^{nor} = P_{GM-CSF}^{nor} T_{GM-CSF} \tag{46}$$

3.7. G-CSF

$$P_{G-CSF}^{endo} = Z\left(\frac{\tilde{w}_{G6}C_{G6} + w_{GRA}C_{GRA}}{\tilde{w}_{G6}C_{G6}^{nor} + w_{GRA}C_{GRA}^{nor}}\right) \tag{47}$$

$$\frac{d}{dt}C_{G-CSF} = P_{G-CSF}^{endo} + P_{G-CSF}^{exo} - C_{G-CSF}\frac{1}{T_{G-CSF}} \tag{48}$$

Again, the quantities $\tilde{w}_{G6}$ and w_{GRA} are hypothetical weighting factors.

Initial value:

$$C_{G-CSF}(0) = C_{G-CSF}^{nor} = P_{G-CSF}^{endo\_nor} T_{G-CSF}^{nor} \tag{49}$$

The quantity P^{exo}_{G-CSF} describes the exogenous influx of administered G-CSF into the G-CSF compartment $P^{exo}_{G-CSF}(0) = 0$. We construct a simple pharmacokinetic model of this process. We assume a delayed release of G-CSF from a subcutaneous compartment, in which the G-CSF has been injected, to the central G-CSF pool (see figure 1). This delay is realized by two subcompartments sc_1 and sc_2.

$$\frac{d}{dt}C_{sc\_1} = -k_{sc}C_{sc\_1} + C^{exo}_{sc} \tag{50}$$

$$\frac{d}{dt}C_{sc\_2} = k_{sc}\left(C_{sc\_1} - C_{sc\_2}\right) \tag{51}$$

$$P^{exo}_{G-CSF} = k_{sc}C_{sc\_2} \tag{52}$$

Initial values:

$$C_{sc\_1}(0) = 0 \tag{53}$$

$$C_{sc\_2}(0) = 0 \tag{54}$$

$$P^{exo}_{G-CSF}(0) = 0 \tag{55}$$

The constant k_{sc} is an equivalent for a transition delay between subcutaneous and central blood compartment. The function C^{exo}_{sc} is equivalent to the applied amount of G-CSF in the time course of the therapy. Let $\{\tilde{t}_i\}$ $(i = 1, \ldots L)$ be the time points of G-CSF administration after the start of the therapy in days $(\tilde{t}_i \geq 0)$, then we obtain

$$C^{exo}_{sc}(t) = d_{G-CSF}\sum_{i=1}^{L}\left(\mathrm{Hv}\left(t - \tilde{t}_i\right) - \mathrm{Hv}\left(t - \tilde{t}_i - t_{inf}\right)\right), \tag{56}$$

where d_{G-CSF} is an equivalent for the administered dose in relation to the normal G-CSF serum concentration, t_{inf} is the duration of infusion and "Hv" is the well known Heaviside function

$$\mathrm{Hv}(t) = \begin{cases} 0 : & t \leq 0 \\ 1 : & t > 0 \end{cases}.$$

Unknown parameters of this pharmacokinetic model (k_{sc} and d_{G-CSF}) were obtained by fitting the model to observed G-CSF serum concentrations after G-CSF administration (see chapter 4).

On the other hand, the degradation of G-CSF is modeled by two independent processes, an unspecific degradation via kidney (e.g. [WSTW], [FOI et al.]) with transit time T^{ren}_{G-CSF} and a specific degradation via granulocytes itself (e.g. [EGGL], [SUF et al.]). This is expressed by a dependence of the quantity T_{G-CSF} on the numbers of blood granulocytes. According to [EGGL], [SUF et al.], we assume a

direct proportionality of granulocytic G-CSF degradation and numbers of granulocytes with factor T^{gra}_{G-CSF}. Recently, this phenomenologically motivated relation has been supported by the analysis of the effects of neutrophil elastase. This enzyme can cleave G-CSF and/or its receptors. Therefore, it seems to be a strong negative feedback mediator of granulopoiesis. Neutrophil elastase is released by blood neutrophils and therefore, the serum level is correlated to the blood neutrophil number ([HDMA], [EFM et al.]).

From the degradation term

$$-\left(\frac{1}{T^{ren}_{G-CSF}}+\frac{1}{T^{gra}_{G-CSF}}C^{rel}_{GRA}\right)C_{G-CSF}$$

it can be obtained that

$$T_{G-CSF}=\frac{T^{ren}_{G-CSF}T^{gra}_{G-CSF}C^{nor}_{GRA}}{T^{ren}_{G-CSF}C_{GRA}+T^{gra}_{G-CSF}C^{nor}_{GRA}} \tag{57}$$

which is a quantity depending on t. The last equation yields the initial (normal) value of T_{G-CSF} which is necessary to calculate (49).

Initial value:

$$T_{G-CSF}\,(0)=T^{nor}_{G-CSF}=\frac{T^{ren}_{G-CSF}T^{gra}_{G-CSF}}{T^{ren}_{G-CSF}+T^{gra}_{G-CSF}}. \tag{58}$$

The relation between the two degradation processes has been chosen in accordance to [SUF et al.], that is, the main degradation of G-CSF is caused by the granulocytes themselves.

The half life of G-CSF in patients after high-dose chemotherapy with extremely low numbers of granulocytes has been directly measured in [SUF et al.] which is a strong experimental evidence for the value of T^{ren}_{G-CSF} (see appendix).

3.8. G

$$C_G=C_{CG}+C_{PGB}+C_{MGB} \tag{59}$$

Initial value:

$$C_G\,(0)=C^{nor}_G=C^{nor}_{CG}+C^{nor}_{PGB}+C^{nor}_{MGB} \tag{60}$$

4. Results

4.1. G-CSF Administration in Healthy Volunteers

Data from a continuous administration of G-CSF in healthy volunteers were taken from the literature ([CPAD], [GRR et al.], [HSS et al.] and [HYT et al.]) and were used to identify unknown parameters related to G-CSF response (see appendix).

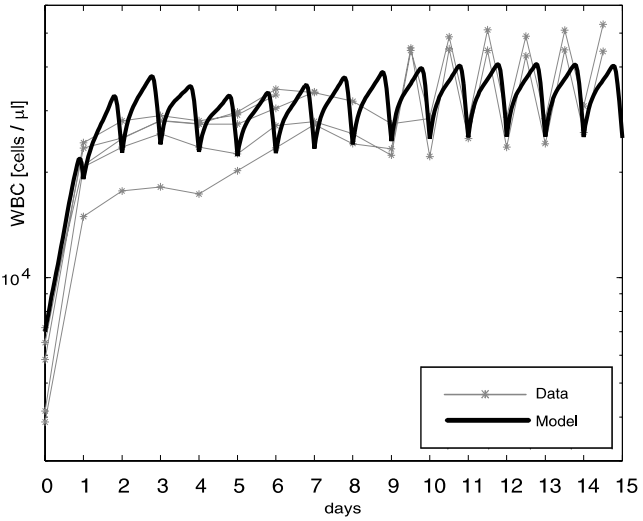

Fig. 2. Repeated daily rhG-CSF application in healthy volunteers.

To simulate repeated daily G-CSF administration, we assume normal initial values and set the sequence of G-CSF administration time points $\{\tilde{t}_i\}$ equal to the sequence $0, 1, \ldots$. We obtain a good fitness of the above data (see figure 2). It is interesting, that the daily fluctuation of granulocytes caused by the rising and falling G-CSF serum concentration after injection, can be modeled exactly. As one can read from the figure, we would expect cell count oscillations very early. Leukocyte counts were collected only once a day at the beginning of the therapy (later twice a day) and therefore, these oscillations could not be detected by the data before day 10.

4.2. Simple Pharmacokinetic Model of G-CSF Application

The construction of a detailed pharmacokinetic model was not our primary objective, however, a realistic influx in our G-CSF compartment is desireable to identify pharmacodynamic parameters.

Data from observed G-CSF serum levels after injection have been taken from the literature ([BBV et al.]). Since the pharmacokinetic and pharmacodynamic behaviour of G-CSF are strictly connected by the assumed degradation mechanism of G-CSF (see section 3.7), the pharmacokinetic parameters k_{sc} and T^{gra}_{G-CSF} were fitted simultaneously to the pharmacokinetic and pharmacodynamic data, that is together with the pharmacodynamic parameters (see section 4.1). This has been done by adding the corresponding fitness functions.

To model the G-CSF serum level data, we are interested in the time dependent behaviour of the corresponding model compartments after daily G-CSF

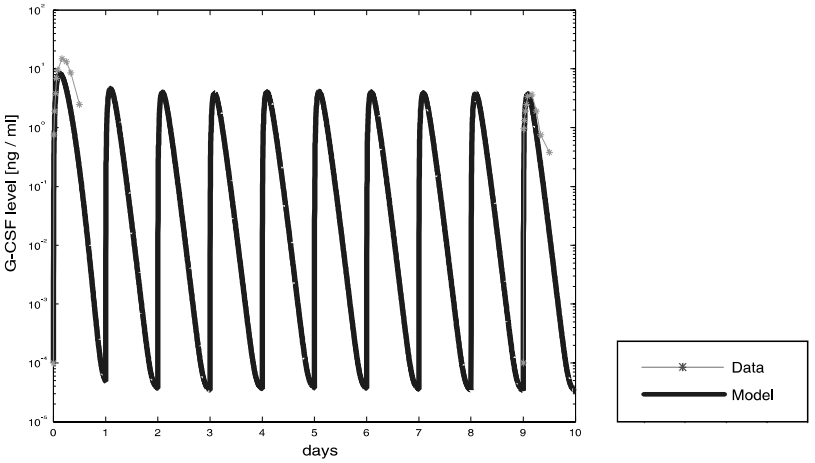

Fig. 3. G-CSF serum levels after repeated daily rhG-CSF injection in healthy volunteers.

administration. The observed G-CSF serum levels could be reproduced by the model (see figure 3).

One can see, that the peak height of G-CSF serum level decreases slightly. Since granulocyte numbers increase rapidly with repeated G-CSF administration (see figure 2), there is a higher degradation of G-CSF at later time points, according to our degradation mechanism via granulocytes (section 3.7). Consequently, G-CSF serum peaks become smaller at later injections. This is a demonstration of the strong relationship between pharmacokinetic and pharmacodynamic properties of G-CSF.

4.3. Modelling of Chemotherapy and Toxicity Estimates

4.3.1. Prescription of Modeled Chemotherapeutic Regimens

We modeled 10 different chemotherapeutic regimens with different dosing and timing schedules of G-CSF, prednisone (Pred) and 5 myelotoxic drugs which are cyclophosphamide (C), doxorubicin (D), vincristine (V), etoposide (E) and procarbazine (P). The drug bleomycin applied in the BEACOPP-regimen has been neglected, because of expected low myelotoxic potential. The following table provides an overview over the different schemes. The doses of cytotoxic drugs were given in mg per m^2 body surface, except for vincristine, where the dose is given in mg. The dose for G-CSF is equal in each regimen ($300\mu g$ if body mass is less than $75kg$ and $480\mu g$ else). The effect of prednisone is considered to be independent from dose for simplicity. We also provide the number of chemotherapy cycles, the time period of repetition and the number of patients.

regimen	G-CSF	C	D	V	E	P	Pred	cycle	remark
CHOP21	-	750	50	2	-	-		6	
(396 patients)		d1	d1	d1			d1-5	d21	
CHOP14		750	50	2	-	-		6	
(393)	d4-13	d1	d1	d1			d1-5	d14	
CHOEP21	-	750	50	2	100	-		6	
(387)		d1	d1	d1	d1-3		d1-5	d21	
CHOEP14		750	50	2	100	-		6	
(398)	d4-13	d1	d1	d1	d1-3		d1-5	d14	
CHOP14		750	50	2	-	-		6/8	only elderly patients
(Ricover, 374)	d6-12	d1	d1	d1			d1-5	d14	($\geq$60 years)
BEACOPP21	-	650	25	2	100	100		8	almost only young
(Basis, 430)		d1	d1	d8	d1-3	d1-7	d1-14	d21	patients (<60 years)
BEACOPP14		650	25	2	100	100		8	only young patients
(82)	d8-13	d1	d1	d8	d1-3	d1-7	d1-8	d14	
BEACOPP21		1250	35	2	200	100		8	only young patients
(escalated, 399)	d8-15	d1	d1	d8	d1-3	d1-7	d1-14	d21	
high-		750–	50/	2	100-	-		6	only young patients,
CHOEP21		1600	27.5–35		200				dose-finding trial
(79)	d6-13	d1	d1/ d1-2	d1	d1-3		d1-5	d21	
high-		750–	50/	2	100-	-		6	only young patients,
CHOEP14		1200	27.5–30		150				dose-finding trial
(39)	d6-13	d1	d1/ d1-2	d1	d1-3		d1-5	d14	

4.3.2. Assumptions Based on Modelling of Data

The myelotoxic effects of chemotherapy can be modeled by setting the sequences for chemotherapy, G-CSF and prednisone injections to appropriate values. We start with normal values except for two cases. In the RICOVER-trial (see section 4.3.1), patients get a pretherapy with vincristine and prednisone which has been modeled by a simulation starting with this pretherapy. As a result, granulocyte level is elevated at the beginning of the therapy (see figure 5), according to data.

Patients treated with BEACOPP-regimen (see section 4.3.1) also show elevated numbers of granulocytes at the beginning of the therapy. This can be understood by an increased G-CSF serum level in the patients caused by lymphoma activity, according to the corresponding group of patients. We model this by a small additional influx of G-CSF into the central G-CSF compartment ($d_{G-CSF} = 20$). Due to the tumour shrinking caused by chemotherapy, this influx declines linearly to zero 80 days after beginning of therapy in the model.

We want to point out two additional assumptions. As has been shown in [WKR et al.], age is a significant prognostic factor for leukopenia. Therefore, we consider two age strata ($\geq$60 years and <60 years). The elderly patients show a significant higher toxicity. Since there is no difference in G-CSF reaction of both strata (see [CPAD]), we expect different toxicity parameters.

Furthermore, we assume a *first cycle effect*, i.e. the toxicity of the first cycle of a multi-cyclic chemotherapy is higher than in further cycles of chemotherapy. The first cycle effect is considered to (primarily) destroy cells which are more sensitive to myelotoxic drugs than others. Even though, in data there is no significant difference in toxicity between first and second cycle, this is, in our opinion, an indirect evidence for the first cycle effect, since the haematopoietic system is not completely (but sufficiently) recovered at the beginning of the second cycle in contrast to the situation at the beginning of the first cycle (steady state). Thus, if there would be no first cycle effect, the myelotoxicity of the second cycle should be higher than that of the first cycle in contradiction to observation. The first cycle effect is modeled by a modification of equation (12):

$$\Psi_{CX}(t) = \begin{cases} f_{fc} & \text{if } (t > t_1) \wedge (t - t_1 \leq 1) \\ 1 & \text{if } \exists i > 1 \ : \ (t > t_i) \wedge (t - t_i \leq 1) \\ 0 & \text{else} \end{cases} \tag{61}$$

which is a constant elevation of toxicity to each cell stage in the first cycle of chemotherapy.

4.3.3. Sensitivity of Parameters and Simulation Based Model Simplification
The question arises whether the toxicity parameters can be estimated separately for each compartment with a sufficient accuracy. This is in fact not always the case.

Model simulations show that the CG-compartment is almost exhausted quickly after beginning of chemotherapy. This can be explained by the damaging process itself and the lower influx from the previous stem cell compartment. Therefore, a greater value for k_{CG} makes no significant greater damage to CG and the k_{CG} can be rised *ad infinitum* without loss of fitness. Figure 4 A and B present the fitness landscape obtained for the CHOP data, varying only k_{CG} and k_{PGB}. Dark areas display parameter values with good fitness with less than 10% deviation from the optimal fit. Such a deviation can hardly be distinguished by eyes if looking at the data. However, a fitness deviation of 20% can be recognized clearly by eye.

On the other hand, if k_{CG} is too small CG recovers too quickly, that is k_{CG} is definitely not zero. Hence, we decided to set always

$$k_{CG} = k_S. \tag{62}$$

If we do the same analysis with the toxicities k_S and k_{PGB}, we obtain a small range of good parameter values for young patients (see figure 4 C). But in some cases, especially for elderly patients, the quantity k_{PGB} can be estimated only with a lower bound (see figure 4 D). On the other hand, the stem cell toxicity k_S is always very sensitive, allowing the determination of a small range of possible values (see next section). The parameter k_{MGB} has a sensitivity between k_S and k_{PGB}. However, the toxicity parameter k_{MGB} has been set to zero for the drugs C, D and V, since there is no evidence for a damage of the corresponding cell stage caused by any of these drugs. Consequently, we fit only two toxicity parameters for these substances.

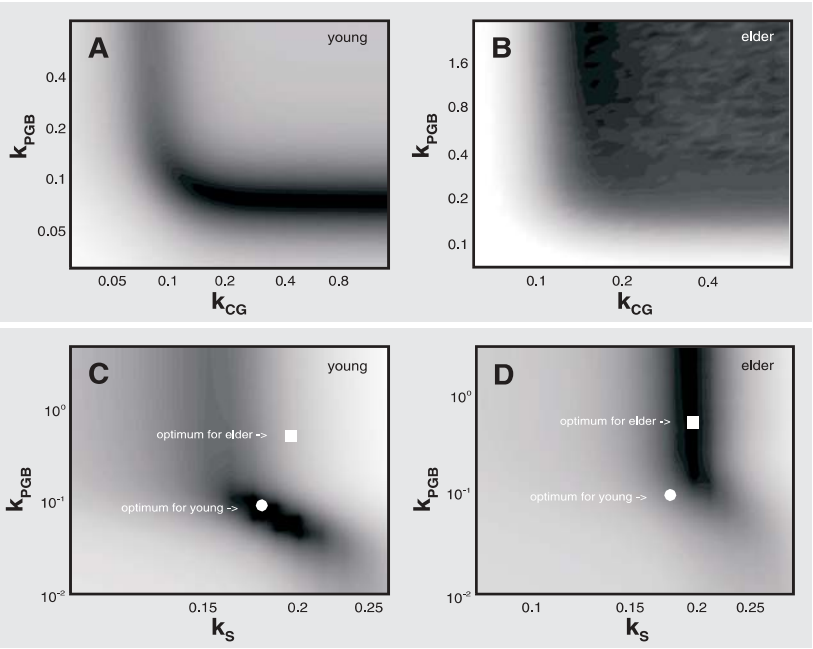

Fig. 4. Fitness landscapes of toxicity parameters obtained from fitting the CHOP data.

Furthermore, an important aspect is the duration of the corresponding drug application, as we find higher sensitivity for parameters related to etoposide or procarbazine which were applied for 3 and 7 days respectively.

Finally, the order of magnitude of a value for a toxicity parameter influences its own sensitivity too, since there is a great difference in model reaction at a parameter range e.g. from 0.01 to 0.1 and there is nearly no difference at a parameter range e.g. from 0.5 to 100. The last one means practically an almost complete exhaustion of the corresponding compartment.

4.3.4. Identified Toxicity Parameters

As already mentioned, toxicity parameters for applied chemotherapeutic drugs can be estimated by fitting the predictions of the model to data of the time course of granulocytes under application of this drug concentration. Of course, it is desirable to estimate the toxicity of single drugs, but to address this issue, the corresponding drug should be administered solitarily or at least in different combinations. Hence, with our data we are unable to distinguish between toxicity proportions related to C and D respectively, since these substances were always applied in combination (see table above). Furthermore, we have data only for the application of drug combinations, so that toxicities for single drugs cannot be estimated by evaluating one chemotherapeutic regimen.

On the other hand, our assumption 8 (see section 1.3) guarantees that the toxicity of a drug combination is the sum of the toxicities of single components. Therefore,

in some cases we are able to identify also the toxicity of single drugs by comparing different chemotherapeutic regimens.

At first, we describe our fitting procedure in detail. Emphasis is placed on the fact that parameters keep unchanged in any further steps after determination in one step:

Step 1. We simultaneously fit the CHOP-data for elderly patients (G-CSF d4-13 and d6-12 (RICOVER)), the pharmacokinetic and the pharmacodynamic data (see section 4.1 and 4.2) to obtain the missing model parameters described in the previous sections as well as the toxicity parameters k_S, k_{PGB} for the drug combination C750+D50+V2 applied in both CHOP regimens. We also estimate the first cycle effect for elderly patients ($f_{fc} = 1.31$) in this step.

Step 2. Using the CHOP data for young patients, we obtain the toxicity parameters k_S, k_{PGB} for the drug combination C750+D50+V2 in this age group as well as the first cycle effect for young patients ($f_{fc} = 1.27$) which can be considered to be equal to that for elderly patients.

Step 3. The CHOEP data can be evaluated to obtain toxicity parameters for E100 which is simply added to the CHOP regimens. This procedure can be done for both age groups.

Step 4. Data from the high-CHOEP dose-finding trial provide the opportunity to estimate dose-toxicity functions for the drug combination C+D and the single drug E in young patients. We assume dose-toxicity functions to be power functions of the dose based on two parameters. Toxicity parameters obtained in previous steps have been used to determine one point of the corresponding dose-toxicity functions, and with it, one of the parameters of the dose-toxicity functions. The effect of vincristine can also be separated by estimating an additive constant (see section 4.3.6. for further details).

Step 5. Toxicity parameters for the drug combinations C650+D25, C1250+D35 and E200 applied in the BEACOPP regimens can be read from the dose-toxicity functions obtained in step 4.

Step 6. Finally, we evaluate the BEACOPP data to estimate the toxicity for P100.

Consequently, we fitted 15 toxicity parameters, including the parameters for the dose-toxicity functions, to model the 9 regimens for young patients. We fitted only 5 toxicity parameters for elderly patients to model the 5 regimens enclosing this age group (see table in section 4.3.1).

The results are demonstrated in the next table. In parenthesis we identify possible ranges of parameters which yield at most 10% deviation from the fitness optimum. We do this only for the first two steps of our fitting procedure, since further parameter ranges depend on the identified optimal values in subsequent adaptions.

drug or drug combination	k_S young	k_S elder	k_{PGB} young	k_{PGB} elder	k_{MGB} young	k_{MGB} elder
C750+D50+V2	**0.1775** (0.17–0.185)	**0.1951** (0.185–0.198)	**0.098** (0.06–0.1)	**0.5** (>0.15)	**0.0** (set)	**0.0** (set)
C650+D25	**0.1229**	no data	**0.024**	no data	**0.0**	no data
C1250+D35	**0.2139**	no data	**0.024**	no data	**0.0**	no data
E100	**0.0030** (0.000–0.007)	**0.0050** (0.004–0.008)	**0.19** (0.06–0.7)	**1** (>0.6)	**0.002** (0.001–0.0035)	**0.005** (0.0025–0.008)
E200	**0.0030**	no data	**0.3**	no data	**0.016**	no data
V2	**0.0385**	no data	**0.073**	no data	**0.0**	no data
P100	**0.0063**	no data	**0.024**	no data	**0.001**	no data

The identified parameters allow some clinically relevant conclusions. The higher myelotoxicity of elderly patients can be explained by a higher sensitivity to chemotherapeutic drugs (higher specific toxicity parameters), instead of a weaker reaction to G-CSF, according to [CPAD]. All other parameters of granulopoiesis have been kept constant in both age groups.

Cyclophosphamide (in combination with doxorubicin) shows a high damaging potential to stem cells according to the literature (e.g. [LS]), but we would expect a low damaging potential to proliferating blasts.

On the other hand, etoposide shows the opposite behaviour, that is, low stem cell toxicity and high toxicity to proliferating blasts. This conforms with current pharmacological knowledge as well (e.g. [ZHK et al.]).

For vincristine we estimated only a small contribution to toxicity which is also a clinical observation.

4.3.5. Simulation Results

In this section we present the simulation results for the various chemotherapy regimens obtained with the estimated set of toxicity parameters.

First we compare the results for young and elderly patients with respect to the same regimen (see figure 5). Further examples can be found in [ESL]. We obtain a good fit for each data set. The higher myelotoxicity of elderly patients, which is indicated by a lower nadir number of WBC (white blood cells), can easily be recognized. Accordingly, the corresponding model curves show a lower minimium caused by the higher toxicity parameters.

The model curve for the CHOP14 (Ricover)-regimen is interesting, since this regimen is essentially the same as the original CHOP14 but with a different G-CSF scheduling. The only change of model parameters with respect to CHOP14 (elderly patients) is the different G-CSF application time interval and the modelling of prednisone pretherapy (see of section 4.3.2.). As one can see, this regimen can be modeled with sufficient accuracy. The prednisone pretherapy causes the beginning of the model curve to be situated at an elevated WBC-level, according to data.

Next, we estimate dose-toxicity functions for the drug combination C+D and the drug E by evaluating data from the dose escalated high-CHOEP regimen in 21

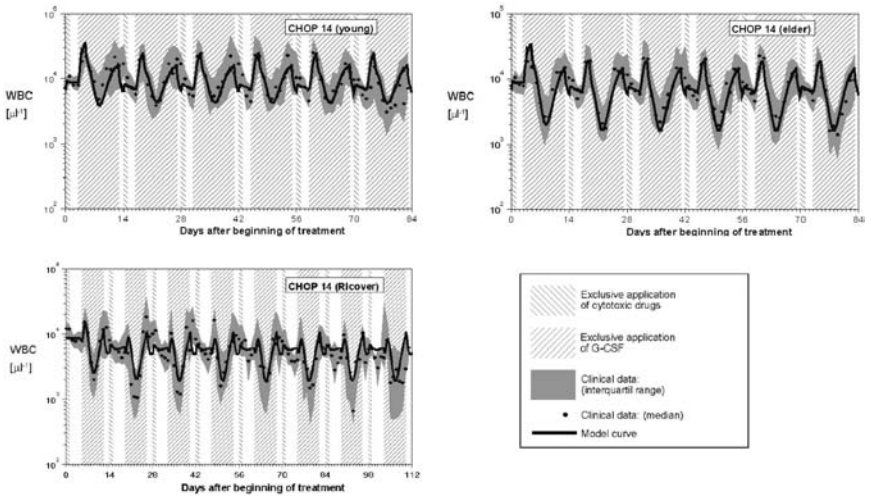

Fig. 5. Comparison between the two age strata of CHOP 14 (G-CSF on day 4 to 13) and CHOP 14 (G-CSF on day 6 to 12 with only elderly patients).

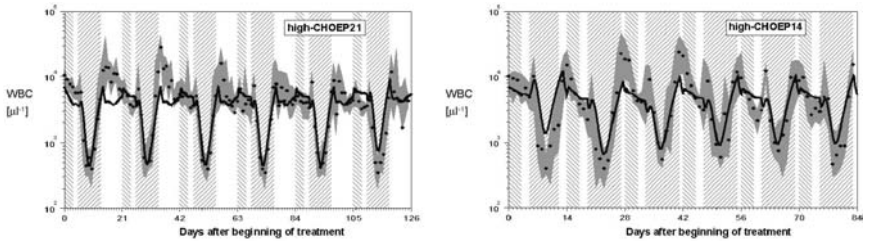

Fig. 6. high-CHOEP regimen, model and data.

and 14 days intervals (see figure 6). Details of this procedure are given in the next section. Using the obtained dose-toxicity functions, we can estimate the toxicity of the drug doses of C+D and E applied in the BEACOPP regimens. With these results, we are able to estimate the toxicity for P by fitting the BEACOPP data (see figure 7, further figures see [ESL]). Finally, notice that the *normalized fitness values*, which are the values of the fitness function divided by the number of cycles, are *essentially the same* (about 30 for the CHO(E)P regimens young and elder, 65 for the BEACOPP regimens and 50 for the high-CHOEP regimens). That is, each regimen is described by our model with nearly the same accuracy. This indicates that the fitness function described in section 1.4 prevents over- or underfitting of the data even with different levels of uncertainty, as expressed by standard error. This is illustrated nicely in the high-CHOEP data. It seems that the peaks of the leukocyte counts are not always reached by the model curves. But, there are higher standard errors in the data, caused by a smaller number of participants in the trial and the inhomogeneity of the applied dose levels. Our fitness function takes the

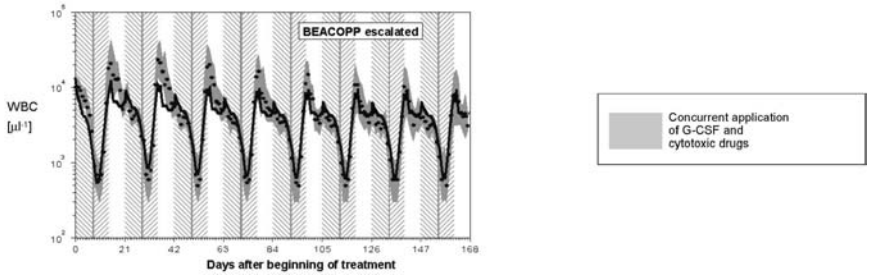

Fig. 7. BEACOPP escalated regimen, model and data.

standard errors into account and one obtains that the normalized fitness value for the high-CHOEP regimen is as good as for example that for the BEACOPP escalated trial which had a much greater number of participants and smaller standard errors.

4.3.6. Dose-Toxicity Functions

The high-CHOEP dose-finding trial is based on a strategy of dose escalation and reduction of the chemotherapeutic drugs applied in the CHOEP regimen, with the aim of estimating tolerable doses with respect to haematotoxicity. Consequently, the administered doses of drugs could change heavily between patients as well as between cycles of one and the same patient. The doses can be changed within the range of 5 prescribed dose levels (from level 4 (highest) to level 0 (standard CHOEP)).

To model this situation, we assume that each patient gets the *median dose level* of the corresponding cycle. For the high-CHOEP21 regimen we obtain the median dose level sequence 4, 3, 3, 3, 3, 2 and for the high-CHOEP14 regimen the dose level sequence 2, 2, 1, 1, 1, 1.

Furthermore, we assume that the toxicity parameters k satisfy

$$k = \beta D_{CX}^{\gamma}, \tag{63}$$

where D_{CX} is the dose of the corresponding drug administered on a single day, β is a proportionality factor and γ can be interpreted as the strength of toxicity increment by increased doses.

As already pointed out, it is not possible to distinguish between toxicity related to C and D, therefore, we consider the dose-toxicity function of C+D only to be a function of the dose of C. Since these two drugs are escalated and reduced in a similar relation, this could be an appropriate way out. On the other hand, from this setting it follows that the obtained toxicity function is at least an upper bound of the toxicity function of single C.

The constants β and γ were fitted. Thereby, in order to reduce the number of parameters, we use the point which already had been obtained from modelling the CHOEP data as fixed points of the functions. Vincristine is always given at a constant dose which can be modeled by an additive constant to the dose-toxicity functions.

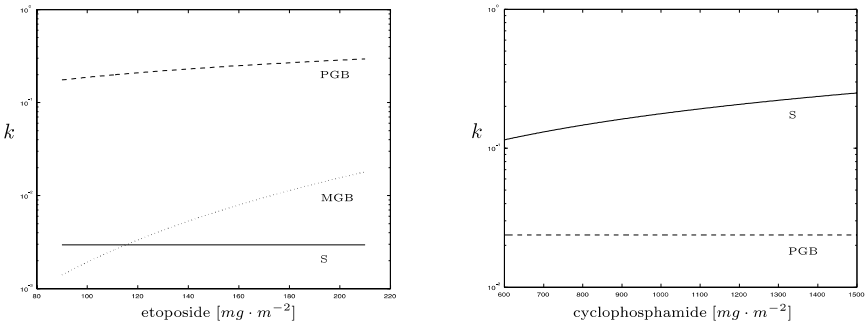

Fig. 8. Dose-toxicity functions for etoposide and cyclophosphamide+doxorubicin.

The simulation results have been shown in the preceding section, here, we want to present the results for the obtained dose-toxicity functions (see figure 8). One can see again that the damaging potential of etoposide to stem cells remains low, even if the dose of etoposide is increased. On the other hand, the toxicity to more mature cells clearly increases with a higher dose. The drug combination cyclophosphamide+doxorubicin shows the opposite behaviour. To quantify the functions in figure 8, we provide a table of the corresponding parameters.

parameter		S	PGB	MGB
etoposide	β	$2.9{\cdot}10^{-3}$	$1.1{\cdot}10^{-2}$	$1.8{\cdot}10^{-9}$
	γ	$4.3{\cdot}10^{-3}$	$6.15{\cdot}10^{-1}$	3.015
cyclophosphamide/	β	$5.08{\cdot}10^{-4}$	$2.4{\cdot}10^{-2}$	0
doxorubicin	γ	$8.474{\cdot}10^{-1}$	$1.5{\cdot}10^{-5}$	-

4.4. Model Response to Single Short Perturbations

After having identified all parameters for our model, we can discuss some aspects of the dynamical behaviour of the model.

First we study the effect of a single G-CSF application to the bone marrow cell stages and the circulating granulocytes. We model a single influx of G-CSF (dose as it is in the chemotherapeutic regimens) at $t = 0$ (see figure 9): One can recognize that the GRA compartment enlarges quickly caused by the G-CSF triggered, increased release of mature granulocytes from the bone marrow (see section 2.7). On the other hand, the GRA compartment is diminished quickly after stimulation because of the fast degradation of G-CSF and the short half life of granulocytes. Since amplification in PGB is stimulated by G-CSF, this compartment is also enlarged. Caused by a lower demand of differentiated cells, stem cells increase their self-renewal probability, and with it, their total number.

Typical system behaviour is an over-compensating of abnormal state variables which leads to a (damped) oscillation of the compartment sizes while approaching

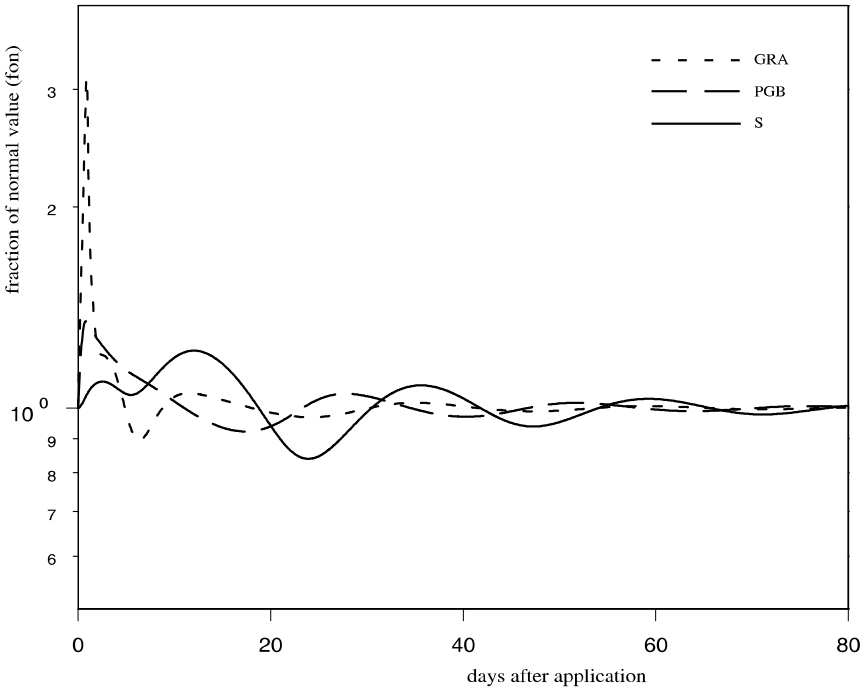

Fig. 9. Model behaviour after single G-CSF application with respect to steady state values.

the steady state. But this behaviour is strongly related to identified parameters. That is, for example, an increment of transit times in MGB to pathological values can lead to stable oscillations of the system as has been modeled in [SFL et al.].

Next we want to study the system behaviour after selective damage of isolated cell stages. Therefore, we either damage only stem cells (one day with $k_S = 0.1$, see figure 10, A) or only proliferating blasts (one day with $k_{PGB} = 0.1$), both at $t = 0$.

Figure 10 illustrates the different reaction of the system to these two damaging mechanisms. Despite a strong depletion of stem cells at the first scenario, the PGB compartment starts to grow. The reason for this is that the CG compartment increases the proliferative fraction in a short term to compensate the expected loss of feeding by the depleted stem cell compartment. As a consequence, the efflux from this compartment increases in the first instance which increases the influx into the PGB compartment. The GRA compartment practically reflects the PGB compartment with a time delay due to the MGB compartment which is also a typical behaviour of this system in case of self-regulation after a single disturbance.

However, the second scenario shows a different behaviour. The strong depletion of the PGB compartment forces the stem cell compartment to decrease the self-renewal probability in order to produce more differentiated cells. This leads to a shrinking of the stem cell pool but also to a quick recovery of the PGB

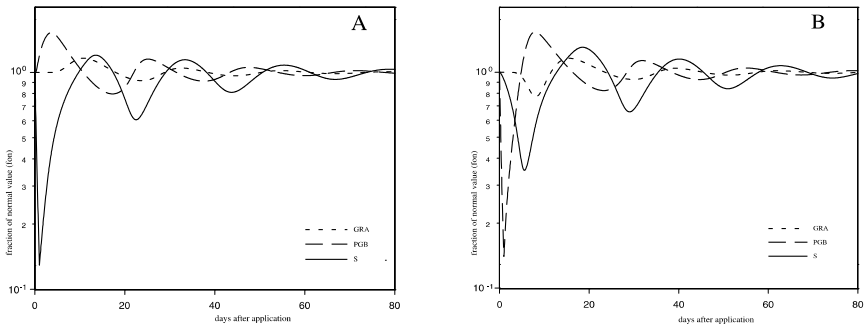

Fig. 10. Model behaviour after cytotoxic drug administration, figure A: only stem cell damage, figure B: only damage to proliferating blasts.

compartment. Again, the GRA compartment is a time delayed reflection of the PGB compartment. In contradiction to a pure stem cell damage, here, the GRA compartment starts to shrink a certain time after the PGB damage.

Of course, a real drug generally damages both cell stages and the reaction of the system is a superposition of the above effects. But, as has been shown, the behaviour of the granulocyte compartment resulting from the application of such a drug can provide information which allows for a distinction between S-toxicity and PGB-toxicity.

4.5. Model Predictions

In this section, we demonstrate how our model can be used to support planning of a new regimen. One criterion to accomplish is clinical feasibility.

Generally, the regimen should result in tolerable haematotoxicity at least with respect to leukocyte count. Clinically, one can define several quantities to validate this criterion. First, the *AOC-value* is the area between the normalized (to 7000 μl^{-1}) time course of leukocytes and the line 4/7 which is defined as the upper bound for a clinical leukopenia (corresponding to 4000 μl^{-1}). This quantity is a measure for the duration and severity of leukopenia and should be as small as possible. Second, the *duration of leukopenia* (DoL) should be small. Thirdly, the *minimum leukocyte count* (MLC) should not drop below a certain level. Finally, the system should be sufficiently recovered on the day of planned continuation of the therapy, therefore, the *minimal recovery value* (MRV) after a completed cycle should also not drop below an appropriate level.

With our model, these quantities can be determined after modelling the corresponding regimen and evaluating the solution for the GRA compartment. However, these quantities are only predictions for the population median and it is not clear, which clinical consequences can be drawn from given absolute values. Therefore, we always compare the quantities calculated for hypothetical regimens with the corresponding ones obtained for the established CHOEP14 regimen, which is known to be rather toxic but feasible for most patients ([PTK2 et al.]), and, request that

new regimens should not be more toxic than this one. We restrict ourselves to the young age group. The next table shows the results from our analysis.

regimen G-CSF	6×CHOEP14 d4-13	6×CHOP14 none	6×CHOP10 d4-9	6×CHOP10 d2-10	6×CHOP11 d5-10
AOC ($[d]$)	3.0	15	4.9	6.1	2.0
DoL ($[h]$)	390	1400	520	580	340
MRV ($[\mu l^{-1}]$)	6100	2200	4300	4800	6100
MLC ($[\mu l^{-1}]$)	1900	1000	1500	1400	2400

With the help of these model predictions, some relevant questions in the context of clinical trials can be discussed.

A question could be if it is possible to safely apply the CHOP regimen with a cycle duration of 14 days (CHOP14) without any supportive G-CSF administration. The answer is likely to be negative, since this regimen is estimated to be much more toxic than CHOEP14 if we compare the third with the second column of the above table (see also figure 11).

Secondly, one could ask if a further time intensification, that is a further shortening of cycle duration, is possible for the CHOP regimen with G-CSF. We simulate a CHOP10 regimen with G-CSF on day 4 to 9. Comparing the second with the fourth column of our table, we can see that this regimen is more toxic than the CHOEP14 regimen but not as toxic as a CHOP14 without G-CSF.

Therefore, one could try to reduce the toxicity in the CHOP10, G-CSF d4-9 regimen by a prolongation of the G-CSF application. But after simulating CHOP10 with G-CSF on day 2 to 10 (fifth column), we obtain that this regimen is even more toxic than the CHOP10 with G-CSF on day 4 to 9. This illustrates that the rule "*much helps much*" is not true in the context of G-CSF application. The main reason for this behaviour is the early loss of the bone marrow reserve pool (see also section 2.7). If G-CSF is applied, the postmitotic apoptosis process will be reduced and the maturation process is accelerated which leads to the release of a greater number of mature bone marrow cells. This results in a very short-termed increment of peripheral neutrophils which can also be recognized in figure 5 for the CHOP14 with G-CSF on day 4-13. Ideally, this release takes place in time of demand, but one has to make a trade-off between exploiting the reserve pool, which also becomes smaller after the beginning of the therapy caused by insufficient supply from earlier cell stages, and, stimulating earlier cell stages just in time, which is necessary for neutrophil recovery.

Since CHOP10 is probably not safe enough, the question arrises if it is possible to shorten the cycle duration for the CHOP regimen at least up to 11 days. Evaluating the last column of our table one can see that with G-CSF application on day 5 to 10, this regimen should be safe. It is estimated to be even less toxic than CHOEP14 (see also figure 11). Finally, we want to estimate how a CHOP21 with G-CSF support can be safely dose-escalated for young patients. Therefore, we use

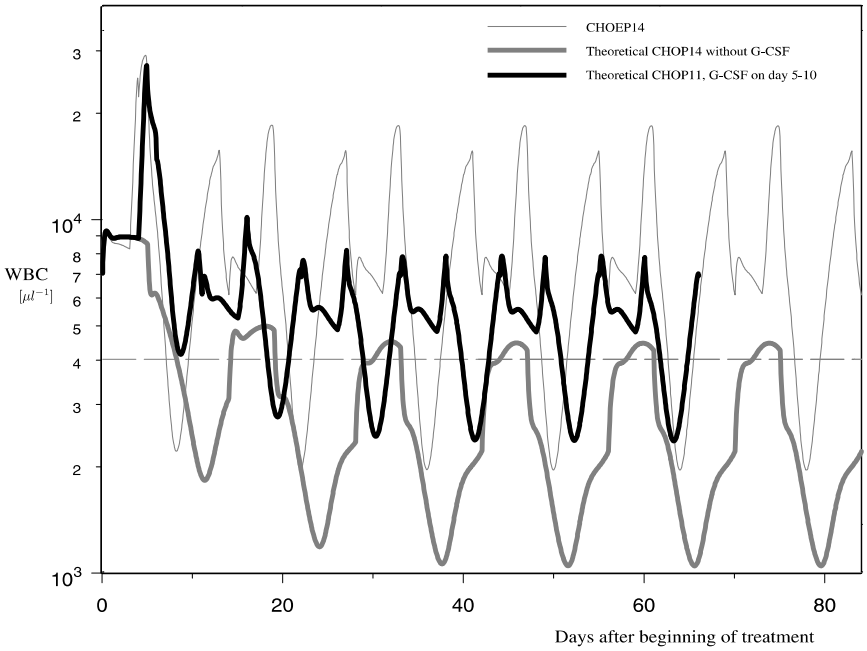

Fig. 11. Comparison of hypothetical regimens with established CHOEP14 based on model calculation, dashed line is upper bound for leukopenia (4000 μl^{-1}).

our dose-toxicity functions for cyclophosphamide and assume a G-CSF application on day 6 to 13 like in the high-CHOEP trials. We obtain functions for our clinical relevant quantities with respect to applied cyclophosphamide dose (see figure 12). We would expect excessive toxicity if cyclophosphamide is applied on a dose above 2300 $mg \cdot m^{-2}$. If we claim that the MRV is at least 2500 μl^{-1}, which is often used as a criterion for therapy continuation, we would estimate that about 2000 $mg \cdot m^{-2}$ is an upper bound for cyclophosphamide application. But of course, this depends on our special G-CSF scheduling.

5. Discussion and Outlook

Our objective was to build a computational model of human granulopoiesis to be applicable to polychemotherapy. We constructed a physiological compartment model to calculate the time course of single identifiable bone marrow cell stages as well as blood cytokine and granulocyte levels after certain disturbances such as chemotherapy. We used a differential equation approach which seems to us appropriate in the context of our objective. The model includes self-regulating mechanisms of the granulopoietic system, describes the effects of G-CSF and steroid applications and the toxic effects of chemotherapeutic drugs as well. To our knowledge, such a model has not been published in the literature so far. A model based on partial differential equations has been proposed recently to simulate the recovery of gran-

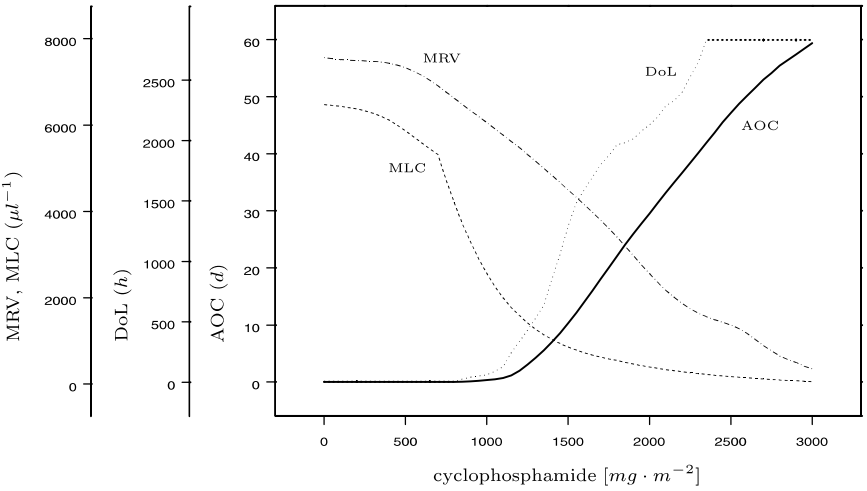

Fig. 12. Estimating clinical quantities for a hypothetical high-CHOP21 regimen with G-CSF on day 6 to 13.

ulopoiesis after high-dose chemotherapy with stem cell transplantation which is not addressed in our paper ([ORKG]).

The basic model structure and regulatory mechanisms of our model were taken from a corresponding model for mice. Since bone marrow data of humans can hardly be obtained, we evaluated peripheral leukocyte counts after application of G-CSF in healthy volunteers, data from large clinical trials and G-CSF pharmacokinetic data to determine unknown model parameters by fitting the predictions of our model to these data. Some of the fitted parameters show a very good agreement with recently measured biological equivalents, such as the normal apoptosis rate in MGB and the amplification in PGB (see appendix). On the other hand, displacements between fitted transit times of single MGB subcompartments ($G4$-$G6$) could be possible (see appendix). We obtained a consistent parameter set, such that all evaluated data can be reproduced by our model with sufficient accuracy.

We constructed a simple pharmacokinetic model of G-CSF based on a delayed influx into the blood after injection and two degradation mechanisms, an unspecific elimination via the kidney and a specific elimination via the granulocytes themselves which both are assumed to be first order kinetics. With it, G-CSF serum concentrations after injections into healthy volunteers could be reproduced. On the other hand, the different pharmacokinetics of novel derivates of G-CSF (e.g. SD/01) keeps unmodeled and is a further objective of our group. In our opinion it is not possible to build a pure pharmacokinetic model of G-CSF without any consideration of its pharmacodynamics, since these properties are strongly linked by the specific degradation mechanism and the G-CSF triggered granulocytosis.

The influence of chemotherapy has been modeled by an instantaneous depletion of cell stages. We assumed a first order kill mechanism which stops after one day. These are rather rough simplifications, since one would expect for example not a

constant kill over time but a diminishing destruction of cells, because of decreasing drug concentrations. On the other hand, for the model recovery dynamics it is more important how many cells are left over after application which can simply be expressed by our toxicity parameters. We assumed no interactions between the cytotoxic drugs, since most of the drugs applied in the regimens considered have different modes of action and act on different stages of the cell cycle or are cell cycle independent ([FP]).

The toxic effects can be quantified by fitting the toxicity parameters to available data. The values of these quantities are measures for the toxic potential of the corresponding drugs or drug combinations to the considered cell stages. Parameters could be obtained for combinations of 5 different chemotherapeutic drugs (cyclophosphamide, doxorubicin, etoposide, procarbazine and vincristine) as well as for single drugs (etoposide, procarbazine, vincristine). The conclusions which can be drawn from the estimated values show a good agreement with clinical observations. On the other hand, we were not always able to assign toxicity parameters to each cell stage. In all cases, the toxicity to CG could be estimated at most with a lower bound because of the strong cell reduction in that compartment, therefore, we assumed it to be equal to the toxicity to S. Sometimes, we had the same problem for the toxicity to PGB. Furthermore, toxicities of different drugs administered at the same time can hardly be seperated, since only a cumulative toxicity is observable. Shifts between the estimated values for toxicity parameters of different drugs but for the same cell stage could be possible in that case. But as a result from our fitting procedure, the data from 10 different chemotherapeutic regimens could be reproduced with our model.

We could explain the higher myelotoxicity of elderly patients by higher values for the toxicity parameters rather than by different granulopoiesis parameters, according to literature ([CPAD]). However, this explanation is not straightforward, since higher estimates for toxicity parameters can have different reasons such as metabolic or pharmacokinetic differences. There are also further risk factors (gender, tumour related factors, health status) which are known to be of significance for myelotoxicity (see [WKR et al.]). In order to provide individually optimal treatments, it could be useful to estimate toxicity parameters with respect to these risk factors. We will address this issue in our further work.

The data from dose-finding trials offer a possibility to estimate dose-toxicity functions for drugs and drug combinations. We estimated two such relations (for etoposide and cyclophosphamide+doxorubicin). Since cyclophosphamide and doxorubicin are applied in combination, we cannot distinguish between toxicity related to these drugs. Therefore, the dose-toxicity function in the latter case is based on the assumption of similiar toxicity increments for both cyclophosphamide and doxorubicin dose escalations.

Some further assumptions had been made to model the chemotherapeutic regimens. We assume a first cycle effect which we estimated to be about 30% more toxic with respect to toxicity parameters than further cycles of the therapy. Without this assumption, by our model the myelotoxicity of the first cycle would be under-estimated in comparison to data. We believe that the biological background of the first cycle effect may be lymphoma related. This kind of tumour is cytokine

releasing and hence makes haematopoiesis somewhat more sensitive to the first treatment.

We neglected the toxicity of bleomycin in the BEACOPP regimens. We assumed equal G-CSF application for each patient with respect to one regimen. Dosage as well as time scheduling are considered to be constant, that is, exceptions from the trial protocol had been neglected. This simplification should be appropriate in every regimen, perhaps except for the BEACOPP escalated regimen ([ELS et al.], [PTK1 et al.], [PTK2 et al.], [WKR et al.]). Similiarly, dose reductions forced by intolerable haematotoxicity had been neglected. But only in the BEACOPP escalated regimen standard dose reductions took place up to a bigger extent ([ELS et al.]).

Our model analysis showed that one could distinguish between stem cell toxicity and toxicity to PGB only by evaluating the peripheral blood granulocytes. Furthermore, the model provides an insight into the bone marrow dynamics after such damages.

Finally, we demonstrated how our model could be used as a tool for the planning of new chemotherapeutic regimen in yet untested dosing and timing schedules to predict the myelotoxic potential and to optimize the administration of G-CSF in that issue. This method is not restricted to lymphomas. It is our future objective to model other chemotherapies of other diseases with the same approach.

Acknowledgements. This paper was supported by the DFG (Deutsche Forschungsgemeinschaft) in the framework of the project "Aufbau von Simulationsmodellen der hämatopoetischen Dynamik nach konventioneller und hochdosierter Chemotherapie und Zytokingabe beim Menschen" (Nr. LO 342/8-2). We would like to thank the *German High Grade Non-Hodgkin's-Lymphoma Study Group* and the *German Hodgkin's Lymphoma Study Group* for the kind provision of data.

References

[BAB et al.] Bishop, C.R., Athens, J.W., Boggs, D.R., Warner, G.E., Cartwright, G.E., Wintrobe, M.M.: A non-steady-state kinetic evaluation of the mechanism of cortisone-induced granulocytosis. J. Clin. Inv., **47**, 249–260 (1968)

[BBB et al.] Busse, D., Busch, F.W., Bohnenstengel, F., Eichelbaum, M., Fischer, P., Opalinska, J., Schumacher, K., Schweizer, E., Kroemer, H.K.: Dose escalation of cyclophosphamide in patients with breast cancer: consequences for pharmacokinetics and metabolism. J. Clin. Oncol. **15** (5), 1885–1896 (1997)

[BBV et al.] Borleffs, J.C.C., Bosschaert, M., Vrehen, H.M., Schneider, M.M.E., van Strijp, J., Small, M.K., Borkett, K.M.: Effect of Escalating Doses of Recombinant Human Granulocyte Colony-Stimulating Factor (Filgrastim) on Circulating Neutrophils in Healthy Subjects. Clinical Therapeutics **20** (4), 722–736 (1998)

[BCMO] Bender, R.A., Castle, M.C., Margileth, D.A., Oliverio, V.T.: The pharmacokinetics of [3H]-vincristine in man. Clin. Pharmacol. Ther. **22** (4), 430–435 (1977)

[BLG et al.] Blayney, D.W., LeBlanc, M.L., Grogan, T., Gaynor, E.R., Chapman, R.A., Spiridonidis, C.H., Taylor, S.A., Bearman, S.I., Miller, T.P., Fisher, R.I.: Dose-Intense Chemotherapy Every 2 Weeks With Dose-Intense Cyclophosphamide, Doxorubicin, Vincristine, and Prednisone May Improve Survival in Intermediate- and High-Grade Lymphoma: A Phase II Study of the Southwest Oncology Group (SWOG 9349). J. Clin. Oncol. **21** (13), 2466–2473 (2003)

[CPAD] Chatta, G.S., Price, T.H., Allen, R.C., Dale, D.C.: Effects of in vivo recombinant methionyl human granulocyte colony-stimulating factor on the neutrophil response and peripheral blood colony-forming cells in healthy young and elderly adult volunteers. Blood **84** (9), 2923–2929 (1994)

[CRP et al.] Colotta, I., Re, F., Polentarutti, N., Sozzani, S., Mantovani, A.: Modulation of granulocyle survival and programmed cell death by cytokines and bacterial products. Blood **80** (8), 2012–2020 (1992)

[DFW] Dale,D.C., Fauci, A.S., Wolff, S.M.: Alternate-day prednisone. T. n. E. J. Med. 1154–1158 (1974)

[E] Engel, C.: Charakterisierung der zellkinetischen Wirkungen von G-CSF auf die Granulopoese, Erythropoese und Stammzellen in der Maus mit Hilfe eines mathematischen Kompartimentmodells. Dissertation, Köln 1999

[EFM et al.] El Ouriaghli, F., Fujiwara, H., Melenhorst, J.J., Sconocchia, G., Hensel, N., Barett, A.J.: Neutrophil elastase enzymatically antagonizes the in vitro action of G-CSF: implications for the regulation of granulopoiesis. Blood **101** (5), 1752–1758 (2003)

[EGGL] Ericson, S.G., Gao, H., Gericke, G.H., Lewis, L.D.: The role of polymorphonuclear neutrophils (PMNs) in clearance of granulocyte colony-stimulating factor (G-CSF) in vivo and in vitro. Exp. Hem. **25** (13), 1313–1325 (1997)

[ELS et al.] Engel, C., Loeffler, M., Schmitz, S., Tesch, H., Diehl, V.: Acute hematologic toxicity and practicability of dose-intensified BEACOPP chemotherapy for advanced stage Hodgkin's disease. German Hodgkin's Lymphoma Study Group (GHSG). Ann. Oncol. **11** (9), 1105–1114 (2000)

[ESL] Engel C., Scholz, M., Loeffler, M.: A computational model of human granulopoiesis to simulate the hematotoxic effects of multicycle polychemotherapy. Blood prepublished June 29, 2004; DOI 10.1182/blood-2004-01-0306

[FOI et al.] Fukuda, M., Oka, M., Ishida, Y., Kinoshita, H., Terashi, K., Kawabata, S., Kinoshita, A., Soda, H., Kohno, S.: Effects of renal function on pharmacokinetics of recombinant human granulocyte colony-stimulating factor in lung cancer patients. Antimicrob Agents Chemother **45** (7), 1947–1951 (2001)

[FP] Ferguson, L.R., Pearson, A.E.: The clinical use of mutagenic anticancer drugs. Mutation Res. **355**, 1–12 (1996)

[GRR et al.] Grigg, A.P., Roberts, A.W., Raunow, H., Houghton, S., Layton, J.E., Boyd, A.W., McGrath, K.M., Maher, D.: Optimizing dose and scheduling of filgrastim (granulocyte colony-stimulating factor) for mobilization and collection of peripheral blood progenitor cells in normal volunteers. Blood **86** (12), 4437–4445 (1995)

[HDMA] Hunter, M.G., Druhan, L.J., Massullo, P.R., Avalos, B.R.: Proteolytic cleavage of granulocyte colony-stimulating factor and its receptor by neutrophil elastase induces growth inhibition and decreased cell surface expression of the granulocyte colony-stimulating factor receptor. Am. J. Hematol. **74** (3), 149–155 (2003)

[HH] Hareng L., Hartung, T.: Induction and Regulation of Endogenous Granulocyte Colony-Stimulating Factor Formation. Biol. Chem. **383**, 1501–1517 (2002)

[HSS et al.] Hoglund, M., Smedmyr, B., Simonsson, B., Totterman, T., Bengtsson, M.: Dose-dependent mobilisation of hematopoietic progenitor cells in healthy volunteers receiving glycosylated rHuG-CSF. Bone marrow transplant **18** (1), 19–27 (1996)

[HYT et al.] Huhn, R.D., Yurkow, E.J., Tushinski, R., Clarke, L., Sturgill, M.G., Hoffmann, R., Sheay, W., Cody, R., Philipp, C., Resta, D., George, M.: Recombinant

human interleukin-3 (rhIL-3) enhances the mobilization of peripheral blood progenitor cells by recombinant human granulocyte colony-stimulating factor (rhG-CSF) in normal volunteers. Exp. Hem. **24** (7), 839–847 (1996)

[LBO et al.] Lord, B.I., Bronchud, M.H., Owens, S., Chang, J., Howell, A., Souza, L., Dexter, M.: The kinetics of human granulopoiesis following treatment with granulocyte colony-stimulating factor in vivo. Proc. Nat. Acad. Sci. USA **86**, Medical Sciences, 9499–9503 (1989)

[LPWW] Loeffler, M., Pantel, H., Wulff, H., Wichmann, H.E.: A mathematical model of erythropoiesis in mice and rats Part 1: Structure of the model. Cell Tissue Kinet. **22**, 13–30 (1989)

[LRO] Lenhoff, S., Rosberg, B., Olofsson, T.: Granulocyte interactions with GM-CSF and G-CSF secretion by endothelial cells and monocytes. European Cytokine Network **10** (4), 525–532 (1999)

[LS] Lohrmann, H.-P., Schreml, W.: Cytotoxic Drugs and the Granulopoietic System. Springer Verlag, Berlin 1982

[MAD] Mackey, M.C., Aprikyan, A.A.G., Dale, D.C.: The rate of apoptosis in post mitotic neutrophil precursors of normal and neutropenic humans. Cell Prolif. **36**, 27–34 (2003)

[ORKG] Ostby, I., Rusten, L.S., Kvalheim, G., Grottum, P.: A mathematical model for reconstitution of granulopoiesis after high dose chemotherapy with autologous stem cell transplantation. J. Math. Biol. **47** (2), 101–136 (2003)

[PCD] Price T.H., Chatta, G.S., Dale, D.C.: Effect of Recombinant Granulocyte Colony-Stimulating Factor on Neutrophil Kinetics in Normal Young and Elderly Humans. Blood **88** (1), 335–340 (1996)

[PTK1 et al.] Pfreundschuh, M., Truemper, L., Kloess, M., Schmits, R., Feller, A.C., Ruebe, C., Rudolph, C., Reiser, M., Hossfeld, D.K., Eimermacher, H., Hasenclever, D., Schmitz, N., Loeffler, M.: 2-weekly or 3-weekly CHOP Chemotherapy with or without Etoposide for the Treatment of Elderly Patients with Aggressive Lymphomas: results of the NHL-B2 trial of the DSHNHL. Blood **104** (3), 634–641 (2004)

[PTK2 et al.] Pfreundschuh, M., Truemper, L., Kloess, M., Schmits, R., Feller, A.C., Rudolph, C., Reiser, M., Hossfeld, D.K., Metzner, B., Hasenclever, D., Glass, B., Ruebe, C., Schmitz, N., Loeffler, M.: 2-weekly or 3-weekly CHOP Chemotherapy with or without Etoposide for the Treatment of Young Patients with Good Prognosis (Normal LDH) Aggressive Lymphomas: results of the NHL-B1 trial of the DSHNHL. Blood **104** (3), 626–633 (2004)

[R] Rechenberg I.: Evolutionsstrategie '94 frommann-holzboog, Stuttgart 1994

[Sch] Schwefel, H.P.: Evolution strategies: A family of nonlinear optimization techniques based on imitating some principles of organic evolution. Ann. Oper. Res. **1**, 65–167 (1984)

[Sin] Sinkule, J.A.: Etoposide: A Semisynthetic Epipodophyllotoxin Chemistry, Pharmacology, Pharmacokinetics, Adverse Effects and Use as an Antineoplastic Agent. Pharmacotherapy **4** (2), 61–73 (1984)

[SFBW] Schmitz, S., Franke, H., Brusis, J., Wichmann, H.E.: Quantification of the cell kinetic effects of G-CSF using a model of human granulopoiesis. Exp. Hem. **21**, 755–760 (1993)

[SFL et al.] Schmitz, S., Franke, H., Loeffler, M., Wichmann, H.E., Diehl, V.: Model analysis of the contrasting effects of GM-CSF and G-CSF treatment on peripheral blood neutrophils observed in three patients with childhood-onset cyclic neutropenia. B. J. Haem. **95**, 616–625 (1996)

[SLJ et al.] Schmitz, S., Loeffler, M., Jones, J.B., Lange, R.D., Wichmann, H.E.: Synchrony of bone marrow proliferation and maturation as the origin of cyclic haematopoiesis. Cell Tissue Kinet. **23**, 425–441 (1990)

[SUF et al.] Shimazaki, C., Uchiyama, H., Fujita, N., Araki, S., Sudo, Y., Yamagata, N., Ashihara, E., Goto, H., Inaba, T., Haruyama, H., Nakagawa, M.: Serum levels of endogenous and exogenous granulocyte colony-stimulating factor after autologous blood stem cell transplantation. Exp. Hem. **23**, 1497–1502 (1995)

[T1] Takahashi, M.: Theoretical basis for cell cycle analysis I. Labelled mitoses wave method. J. Theo. Biol. **13**, 202–211 (1966)

[T2] Takahashi, M.: Theoretical basis for cell cycle analysis II. Further studies on labelled mitosis wave method. J. Theo. Biol. **18**, 195–209 (1968)

[WKR et al.] Wunderlich, A., Kloess, M., Reiser, M., Rudolph, C., Trümper, L., Bittner, S., Schmalenberg, H., Schmits, R., Pfreundschuh, M., Loeffler, M.: Practicability and acute haematological toxicity of 2- and 3-weekly CHOP and CHOEP chemotherapy for aggressive non-Hodgkin lymphoma: results from the NHL-B trial of the German High-Grade Non-Hodgkin's Lymphoma Study Group (DSHNHL). Ann. Oncol. **14** (6), 881–893 (2003)

[WL] Wichmann, H.-E., Loeffler, M.: Mathematical Modeling of Cell Proliferation: Stem Cell Regulation in Hemopoiesis. CRC Press, Boca Raton 1985

[WSTW] Wu, W., Sun, G., Tian, G., Wang, Z.: Serum granulocyte colony-stimulating factor in patients with chronic renal failure. Chin. Med. J. **114** (6), 596–599 (2001)

[ZHK et al.] Zelenetz, A.D., Hamlin, P., Kewalramani, T., Yahalom, J., Nimer, S., Moskowitz, C.H.: Ifosfamide, carboplatin, etoposide (ICE)-based second-line chemotherapy for the management of relapsed and refractory aggressive non-Hodgkin's lymphoma. Ann. Oncol. **14**, 5–10 (2003)

A. Appendix: Parameter Settings

We skip toxicity parameters in this part, since we have already diskussed them in chapter 4. Not regulated quantities are specified with single normal values.

A.1. S

parameter/quantity	value	source
τ_S	8h	[WL], p. 70
p_δ	0.1	”
a_S^{min}	0.01	”
a_S^{nor}	0.15	”
a_S^{int}	0.45	”
a_S^{max}	1	”
ϑ_E	-2	”
ϑ_G	-8	”
ω_S	1	”
ω_G	0.1	”
ω_E	0.3	”

A.2. CG

parameter/quantity	value	source
a_{CG}^{min}	0.3	[WL], p. 71
a_{CG}^{nor}	0.33	”
a_{CG}^{int}	0.66	”
a_{CG}^{max}	1	”
A_{CG}^{min}	1	set
A_{CG}^{nor}	64	[SFBW]
A_{CG}^{max}	333	fitted
$b_{A_{CG}}$	0.4	”
T_{CG}^{nor}	112h	[SFBW]

A.3. PGB

parameter/quantity	value	source
a_{PGB}^{nor}	1	[WL], p. 73
A_{PGB}^{min}	4	set
A_{PGB}^{nor}	32	[PCD], [SFBW]
A_{PGB}^{max}	330	”
$b_{A_{PGB}}$	0.27	fitted
T_{PGB}^{nor}	148h	[SFBW]

A.4. MGB

A.4.1. G4

parameter/quantity	value	source
N_{G4}	5	set
A_{G4}^{nor}	1	”
T_{G4}^{min}	60h	”
T_{G4}^{nor}	51h	fitted
T_{G4}^{max}	1h	”
$b_{T_{G4}}$	0.845	”

A.4.2. G5

parameter/quantity	value	source
N_{G5}	5	set
A_{G5}^{nor}	1	”
T_{G5}^{min}	100h	”
T_{G5}^{nor}	92h	fitted
T_{G5}^{max}	46h	”
$b_{T_{G5}}$	0.845	”

A.4.3. G6

parameter/quantity	value	source
N_{G6}	5	set
A_{G6}^{min}	0.01	”
A_{G6}^{nor}	0.4277	fitted, [MAD]
A_{G6}^{max}	1	set
$b_{A_{G6}}$	1.52	fitted
T_{G6}^{min}	140h	set
T_{G6}^{nor}	22h	fitted
T_{G6}^{max}	20h	”
$b_{T_{G6}}$	0.845	”

A.5. GRA

parameter/quantity	value	source
T_{GRA}^{nor}	5h	[SFBW]
T_{GRA}^{Pred}	0.66	[DFW]

A.6. GM-CSF

parameter/quantity	value	source
P^{max}_{GM-CSF}	0.91h^{-1}	fitted
P^{nor}_{GM-CSF}	1h^{-1}	normalization
P^{min}_{GM-CSF}	310h^{-1}	fitted
$b_{P_{GM-CSF}}$	1.7	”
T_{GM-CSF}	2h	set
w_{CG}	1	”
w_{PGB}	1	”
w_{G4}	1	”
w_{G5}	1	”
w_{G6}	0.2	”

A.7. G-CSF

parameter/quantity	value	source
P^{max}_{G-CSF}	0.97h^{-1}	fitted
P^{nor}_{G-CSF}	1h^{-1}	normalization
P^{min}_{G-CSF}	410h^{-1}	fitted
$b_{P_{GM-CSF}}$	0.33	”
k_{sc}	0.75	”
d_{G-CSF}	$5.6 \cdot 10^6$	”
t_{inf}	2min	set
T^{ren}_{G-CSF}	20h	fitted, [SUF et al.]
T^{gra}_{G-CSF}	2.8h	fitted
$\tilde{w}_{G6}$	0.2	set
w_{GRA}	1	”

Remarks:

1. The amplification in PGB has been fitted, but now the data in [PCD] can be reproduced. Hence, we assume one additional mitosis in steady state and only three to four additional mitoses under G-CSF stimulation in comparison to [SFBW].
2. The parameters A^{nor}_{G6} and T^{ren}_{G-CSF} have also been fitted but show a very good agreement with the literature ([MAD], [SUF et al.] regarding the relation between half life and transit time).
3. The sum of the quantities T^{nor}_{G4}, T^{nor}_{G5} and T^{nor}_{G6} is equal to the sum of these quantities estimated in [SFBW] and in accordance to [PCD]. Due to the fact,

that the total transit time of cells through MGB has a much lesser uncertainty than the transit times of the subcompartments $G4$, $G5$ and $G6$, we fixed the sum but adjusted the single terms of the sum. The same is true for the corresponding min- and max-values ([LBO et al.], [PCD]), but, displacements between the contributions of $G4$, $G5$ and $G6$ to the sum of these quantities are possible.

4. We have chosen 5 subcompartments for each of the compartments $G4$, $G5$, and $G6$. From section 2.6 it follows that with this setting and under steady state conditions, the variances of the transit times have been estimated to be $500h^2$, $1700h^2$ and $100h^2$ respectively (rounded values).
5. Even though, the sensitivity parameter for the transit time has been fitted, it is assumed to be equal in every subcompartment of MGB to reduce the number of unknown parameters.
6. Generally, data for Y^{min}-quantities have a greater uncertainty, since these values are hardly underpinned with measurements.